Chem. Res. Toxicol. 2004, *17*, 1750 1756

Oxidative DNA Damage Induced by Carcinogenic Dinitropyrenes in the Presence of P450 Reductase

Mariko Murata,[†] Shiho Ohnishi,[†] Kazuharu Seike,[†] Kiyoshi Fukuhara,[‡] Naoki Miyata,[§] and Shosuke Kawanishi*[,†]

Department of Environmental and Molecular Medicine, Mie University School of Medicine, 2-174, Edobashi, Tsu, Mie 514-8507, Japan, National Institute of Health Science, 1-18-1, Kamiyouga Setagaya-ku, Tokyo 158-8501, Japan, and Department of Graduate School of Pharmaceutical Sciences, Nagoya City University, 3-1 Tanabe-dori, Mizuho-ku, Nagoya, Aichi 467-8603, Japan

Received September 2, 2004

Nitropyrenes are widespread in the environment due to mainly diesel engine emissions. Dinitropyrenes (DNPs), especially 1,8-dinitropyrene (1,8-DNP) and 1,6-dinitropyrene (1,6-DNP), are much more potent mutagens than other nitropyrenes. The carcinogenicity of 1,8-DNP and 1,6-DNP is stronger than 1,3-dinitropyrene (1,3-DNP). It is considered that adduct formation after metabolic activation plays an important role in the expression of carcinogenicity of nitropyrenes. However, Djuric et al. [(1993) *Cancer Lett.*] reported that oxidative DNA damage was also found as well as adduct formation in rats treated with 1,6-DNP. We investigated oxidative DNA damage by DNPs in the presence of NAD(P)H-cytochrome P450 reductase using ^{32}P-5′-end-labeled DNA. After P450 reductase treatment, DNPs induced Cu(II)-mediated DNA damage in the presence of NAD(P)H. The intensity of DNA damage by 1,8-DNP or 1,6-DNP was stronger than 1,3-DNP. We also examined synthetic 1-nitro-8-nitrosopyrene (1,8-NNOP) and 1-nitro-6-nitrosopyrene (1,6-NNOP) as one of the metabolites of 1,8-DNP and 1,6-DNP, respectively, to find that 1,8-NNOP and 1,6-NNOP induced Cu(II)-mediated DNA damage in the presence of NAD(P)H but untreated DNPs did not. In both cases of P450 reductase-treated DNPs and NNOPs, catalase and a Cu(I) specific chelator attenuated DNA damage, indicating the involvement of H_2O_2 and Cu(I). Using a Clarke oxygen electrode, oxygen consumption by the reaction of NNOPs with NAD(P)H and Cu(II) was measured to find that NNOP was nonenzymatically reduced by NAD(P)H and that the addition of Cu(II) promoted the redox cycle. Therefore, these results suggest that DNPs are enzymatically reduced to NNOPs via nitro radical anion and that NNOPs are further reduced nonenzymatically by NAD(P)H. Subsequently, autoxidation of nitro radical anion and the reduced form of NNOP occurs, resulting in O_2^- generation and DNA damage. We conclude that oxidative DNA damage in addition to DNA adduct formation may play important roles in the carcinogenesis of DNPs via their metabolites.

Introduction

Nitropolycyclic aromatic hydrocarbons including nitropyrenes (NPs) are widespread in the environment due to mainly diesel engine emissions (*1*, *2*). NPs are strongly mutagenic in the bacterial mutation assay (Ames test) and human cell mutagenicity assay (*3*, *4*). Dinitropyrenes (DNPs),[1] especially 1,8-dinitropyrene (1,8-DNP) and 1,6-dinitropyrene (1,6-DNP), are much more potent mutagens than other nitropyrenes. DNPs induced lung cancer and leukemia in rodents. An epidemiological study demonstrated that significant positive trends in lung cancer risk were observed with increasing cumulative exposure of diesel exhaust in male truck drivers (*5*). The International Agency for Research on Cancer (IARC) has assessed that 1,8-DNP and 1,6-DNP have been possibly carcinogenic to humans (group 2B), whereas 1,3-dinitropyrene (1,3-DNP) has not been classifiable as to its carcinogenicity to humans (group 3) (*1*).

Chemical mutagenesis is strongly affected by metabolic activation. Cellular nitroreductase and *O*-acetyltransferase activities have been shown to markedly influence the genotoxic activity of nitro-aromatic compounds (*6*). DNA adduct formation after metabolic activation has been considered to be a major causal factor of carcinogenesis by DNPs. DNPs undergo nitroreduction to *N*-hydroxy arylamines that bind to DNA directly or after *O*-esterification (*1*). DNP adducts are identified as *N*-(deoxyguanosin-8-yl)amino-nitropyrene (dG-C8-1,6-ANP and dG-C8-1,8-ANP), leading to mutation and carcinogenesis (*1*, *7*). On the other hand, Djuric et al. found not only DNA adducts but also oxidative DNA damage in rats

* To whom correspondence should be addressed. Tel/Fax: +81-59-231-5011. E-mail: kawanisi@doc.medic.mie-u.ac.jp.
† Mie University School of Medicine.
‡ National Institute of Health Science.
§ Nagoya City University.

[1] Abbreviations: DNPs, dinitropyrenes; 1,3-DNP, 1,3-dinitropyrene; 1,6-DNP, 1,6-dinitropyrene; 1,8-DNP, 1,8-dinitropyrene; NNOPs, nitronitrosopyrenes; 1,6-NNOP, 1-nitro-6-nitrosopyrene; 1,8-NNOP, 1-nitro-8-nitrosopyrene; 8-oxodG, 8-oxo-7,8-dihydro-2′-deoxyguanosine; NAD(P)H, β-nicotinamide adenine dinucleotide (phosphate) (reduced form); P450 reductase, NAD(P)H-cytochrome P450 reductase; O_2^-, superoxide; ECD, electrochemical detector; DTPA, diethylenetriamine-*N*,*N*,*N*′,*N*″,*N*″-pentaacetic acid; SOD, superoxide dismutase.

10.1021/tx0497550 CCC: $27.50
Published on Web 11/24/2004

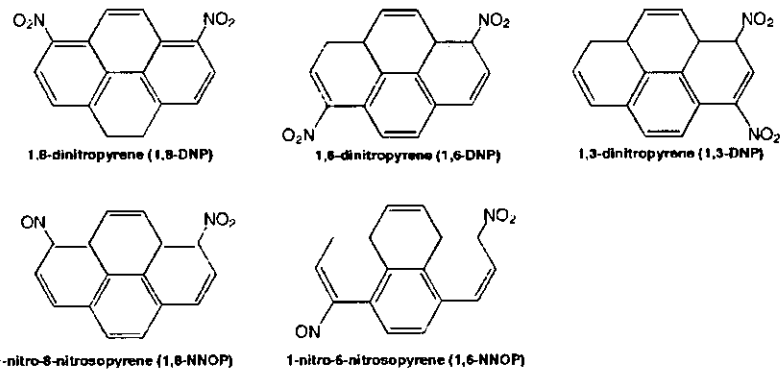

Figure 1. Chemical structures of DNPs and their metabolites used in this study.

treated with 1,6-DNP (*8*). Furthermore, we previously revealed the role of a nitroso derivative of 1-nitropyrene on causing oxidative DNA damage (*9*). It has been reported that nitro-nitroso derivatives are metabolic intermediates of DNPs during metabolic activation, which are more mutagenic than their parent DNPs (*10*). These indicate that oxidative DNA damage by DNPs after metabolic activation plays a role in carcinogenesis.

In this study, we investigated oxidative DNA damage induced by DNPs in the presence of NAD(P)H-cytochrome P450 reductase (P450 reductase), using ^{32}P-5′-end-labeled DNA fragments obtained from the human *p53* and *p16* tumor suppressor genes and the c-Ha-*ras*-1 protooncogene. We also examined synthetic nitro-nitrosopyrenes (NNOP), 1-nitro-8-nitrosopyrene (1,8-NNOP), and 1-nitro-6-nitrosopyrene (1,6-NNOP) as nitroso metabolites of DNP. The chemical structures of DNPs and synthetic NNOPs used in this study are shown in Figure 1. We also analyzed 8-oxo-7,8-dihydro-2′-deoxyguanosine (8-oxodG) formation in calf thymus DNA.

Materials and Methods

Materials. 1,6-NNOP and 1,8-NNOP were synthesized by oxidation of 1-nitro-6-aminopyrene and 1-nitro-8-aminopyrene, respectively, according to the method by the reference (*11*). The nitroaminopyrene used in the synthesis was carried out until none of the undesired isomer could be detected by ^{1}H NMR spectroscopy. To a solution of the purified aminonitropyrene dissolved in CH_2Cl, a solution of *m*-CPBA in CH_2Cl was added dropwise over 20 min and the reaction was carried out at 5 °C for 4 h. The mixture was washed with saturated $NaHCO_3$ and brine, and the organic phase was dried over anhydrous Na_2SO_4. Following evaporation in vacuo, the product was obtained by column chromatography on silica gel using *n*-hexanes–ethyl acetate as the eluent and further recrystallization from *n*-hexanes–ethyl acetate to produce light orange crystals. The purity of each compound was >99% as assessed by ^{1}H NMR spectroscopy.

1. 1,6-NNOP. ^{1}H NMR (400 MHz DMSO-d_6): δ 7.04 (1H, d, *J* = 8.8 Hz), 8.49 (1H, d, *J* = 8.8 Hz), 8.64 (1H, d, *J* = 9.2 Hz), 8.84 (1H, d, *J* = 8.4 Hz), 8.92 (1H, d, *J* = 8.4 Hz), 8.97 (1H, d, *J* = 9.6 Hz), 9.00 (1H, d, *J* = 9.2 Hz), 10.42 (1H, d, *J* = 9.6 Hz), mp 244 °C (decomp.) [lit. (*11*) >233 °C (decomp.)].

2. 1,8-NNOP. ^{1}H NMR (400 MHz DMSO-d_6): δ 7.03 (1H, d, *J* = 8.4 Hz), 8.49 (1H, d, *J* = 8.4 Hz), 8.55 (1H, d, *J* = 8.8 Hz), 8.71 (1H, d, *J* = 8.8 Hz), 8.75 (1H, d, *J* = 8.8 Hz), 8.92 (1H, d, *J* = 8.8 Hz), 9.21 (1H, d, *J* = 9.6 Hz), 10.45 (1H, d, *J* = 9.6 Hz), mp 268 °C (decomp.) [lit. (*11*) > 245 °C (decomp.)].

Restriction enzymes (*Hind* III, *Sty* I, *Apa* I, *Acc* I, and *Xba* I) and T_4 polynucleotide kinase were purchased from New England Biolabs (Beverly, MA). [γ-^{32}P]ATP (222 TBq/mmol) was obtained from New England Nuclear. Alkaline phosphatase from calf intestine was purchased from Roche Molecular Biochemicals (Mannheim, Germany). 1,8-DNP, 1,6-DNP, and 1,3-DNP were purchased from Aldrich Chemical Co. (Milwaukee, IL; the purities were 98, 98, and 99%, respectively). P450 reductase from rat microsome was a kind gift from Prof. Y. Kumagai (Tsukuba University). Piperidine was purchased from Wako Chemical Industries Ltd. (Osaka, Japan). Copper(II) chloride dihydrate was purchased from Nacalai Tesque, Inc. (Kyoto, Japan). Diethylenetriamine-*N*,*N*,*N*′,*N*″,*N*″-pentaacetic acid (DTPA) and bathocuproinedisulfonic acid were purchased from Dojin Chemicals Co. (Kumamoto, Japan). Calf thymus DNA, superoxide dismutase (SOD) (3000 units/mg from bovine erythrocytes), and catalase (45000 units/mg from bovine liver) were purchased from Sigma Chemical Co. (St. Louis, MO). Nuclease P_1 (400 units/mg) was purchased from Yamasa Shoyu Co. (Chiba, Japan).

Preparation of ^{32}P-5′-End-Labeled DNA Fragments Obtained from the *p53* Gene, the *p16* Gene, and the c-Ha-*ras*-1 Gene. DNA fragments were obtained from the human *p53* and *p16* tumor suppressor gene (*12*, *13*) and the c-Ha-*ras*-1 protooncogene (*14*). A singly ^{32}P-5′-end-labeled double-stranded 443 bp fragment (*Apa* I 14179-*Eco* RI* 14621) from the *p53* gene was prepared from the pUC18 plasmid according to a method described previously (*15*). A singly labeled 328 bp fragment (*Eco*RI*5841-*Mro*I 6168) of the *p16* gene was prepared from pGEM-T Easy Vector (Promega Corporation) as described previously (*16*). A 261 bp fragment (*Acc* I* 1645-*Xba* I 1905) and a 341 bp fragment (*Xba*I 1906-*Acc*I* 2246) from the c-Ha-*ras*-1 gene were prepared from plasmid pbcN1, which carries a 6.6 kb *Bam*H I chromosomal DNA restriction fragment as described previously (*17*). The asterisk indicates ^{32}P labeling.

Detection of DNA Damage. A standard reaction mixture (in a microtube; 1.5 mL) contained $CuCl_2$, NADPH, NNOP, ^{32}P-5′-end-labeled double-stranded DNA fragments, and calf thymus DNA in 200 μL of 10 mM sodium phosphate buffer (pH 7.8). For nitroreduction, DNP, 100 μM NADPH, and P450 reductase were preincubated at 25 °C for 30 min in 20 mM potassium phosphate buffer (pH 7.4). After the preincubation, ^{32}P-labeled DNA fragments, calf thymus DNA, and $CuCl_2$ were added to the mixtures (total 200 μL), followed by the incubation. After incubation at 37 °C for 1 h, DNA fragments were treated in 10% (v/v) piperidine at 90 °C for 20 min or treated with 6 units of Fpg protein in reaction buffer [10 mM HEPES–KOH (pH 7.4), 100 mM KCl, 10 mM EDTA, and 0.1 mg/mL BSA] at 37 °C for 2 h, as described previously (*18*). The treated DNA fragments were electrophoresed on an 8% polyacrylamide/8 M urea gel, and an autoradiogram was obtained by exposing X-ray film to the gel. To make the dose of DNA constant, we used calf thymus DNA (20–50 μM) at an excessive dose as compared with ^{32}P-labeled DNA (less than pM) that can be negligible, because the required dose of ^{32}P-labeled DNA, for detection of DNA damage, varies according to the decaying radioactivity (^{32}P; $T_{1/2}$ = 14 days). The preferred cleavage sites were determined by direct comparison of the positions of the oligonucleotides with those produced by the chemical reactions of the Maxam–Gilbert

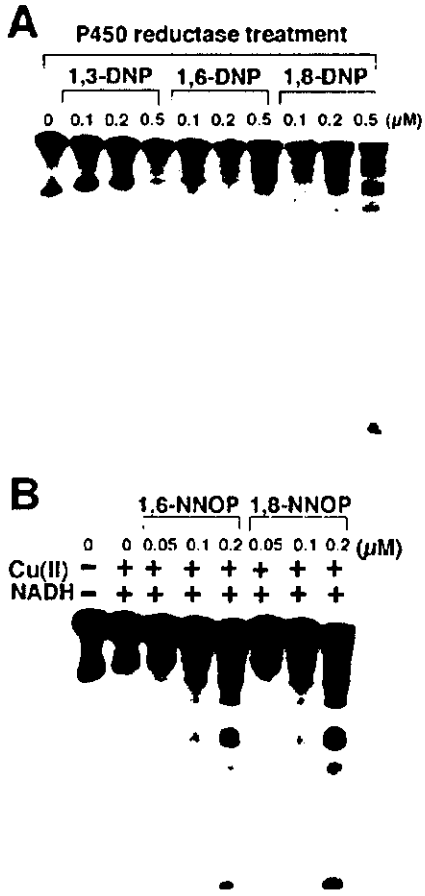

Figure 2. Autoradiogram of ^{32}P-labeled DNA fragment treated with DNPs and their nitro-nitroso derivatives. (A) The reaction mixtures containing the indicated concentrations of DNPs, 100 μM NADPH, and 2.1 μg/mL P450 reductase were preincubated at 25 °C for 30 min in potassium phosphate buffer (pH 7.4). After preincubation, a ^{32}P-5′-end-labeled 328 bp DNA fragment, calf thymus DNA (20 μM/base), and 20 μM $CuCl_2$ were added to the mixtures. (B) The reaction mixture contained a ^{32}P-5′-end-labeled 341 bp DNA fragment, calf thymus DNA (50 μM/base), the indicated concentrations of 1,8-NNOP or 1,6-NNOP, 100 μM NADH, and 20 μM $CuCl_2$ in sodium phosphate buffer (pH 7.8). The reaction mixtures were incubated at 37 °C for 1 h, followed by piperidine treatment, as described in the Materials and Methods. The DNA fragments were electrophoresed on an 8% polyacrylamide/8 M urea gel, and an autoradiogram was obtained by exposing an X-ray film to the gel.

procedure (*19*) using a DNA sequencing system (LKB 2010 Macrophor). A laser densitometer (LKB 2222 UltroScan XL) was used for the measurement of the relative amounts of oligonucleotides from the treated DNA fragments.

Analysis of 8-OxodG Formation by DNPs and NNOPs. The calf thymus DNA fragment was incubated with NNOP or treated DNP, NAD(P)H, and $CuCl_2$. After ethanol precipitation, DNA was digested to its component nucleosides with nuclease P_1 and calf intestine phosphatase and analyzed by HPLC-electrochemical detector (ECD), as described previously (*20*).

Measurement of Oxygen Consumption. Oxygen consumption by the reaction of NNOPs with NADH and $CuCl_2$ was measured using a Clarke oxygen electrode (Electronic Stirrer model 300, Rank Brothers Ltd., Bottisham Cambridge, United Kingdom). The reactions were performed in a mixture containing NNOP, NADH, and $CuCl_2$ in 2 mL of 10 mM phosphate buffer (pH 7.8) containing 2.5 μM DTPA at 37 °C. Catalase was added in order to detect H_2O_2 generation due to oxygen consumption.

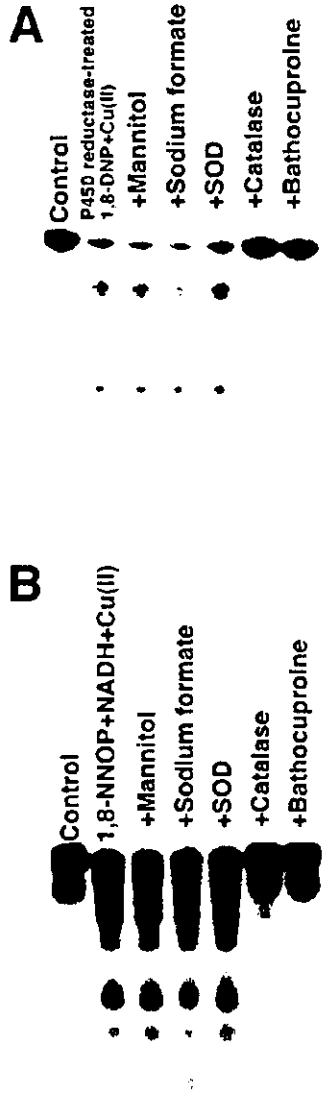

Figure 3. Effects of scavengers and bathocuproine on Cu(II)/NAD(P)H-mediated DNA damage induced by P450 reductase-catalyzed 1,8-DNP and 1,8-NNOP. (A) The reaction mixtures containing 0.5 μM 1,8-DNP, 100 μM NADPH, and 2.1 μg/mL P450 reductase were preincubated at 25 °C for 30 min in potassium phosphate buffer (pH 7.4). After preincubation, a ^{32}P-5′-end-labeled 309 bp DNA fragment, calf thymus DNA (20 μM/base), 20 μM $CuCl_2$, and a scavenger were added to the mixtures. (B) The reaction mixture contained a ^{32}P-5′-end-labeled 261 bp DNA fragment, calf thymus DNA (20 μM/base), 0.2 μM 1,8-NNOP, 20 μM $CuCl_2$, and a scavenger in sodium phosphate buffer (pH 7.8). The reaction mixtures were incubated at 37 °C for 1 h, followed by piperidine treatment. The DNA fragments were analyzed as described in the legend to Figure 2. The concentrations of scavengers and bathocuproine were as follows: 0.1 M mannitol, 0.1 M sodium formate, 30 units of SOD, 30 units of catalase, and 50 μM bathocuproine.

Results

Damage to ^{32}P-Labeled DNA. Figure 2 shows an autoradiogram of a DNA fragment treated with DNPs and NNOPs. Oligonucleotides were detected on the autoradiogram as a result of DNA damage. DNPs did not cause DNA damage in the presence of NAD(P)H and Cu-

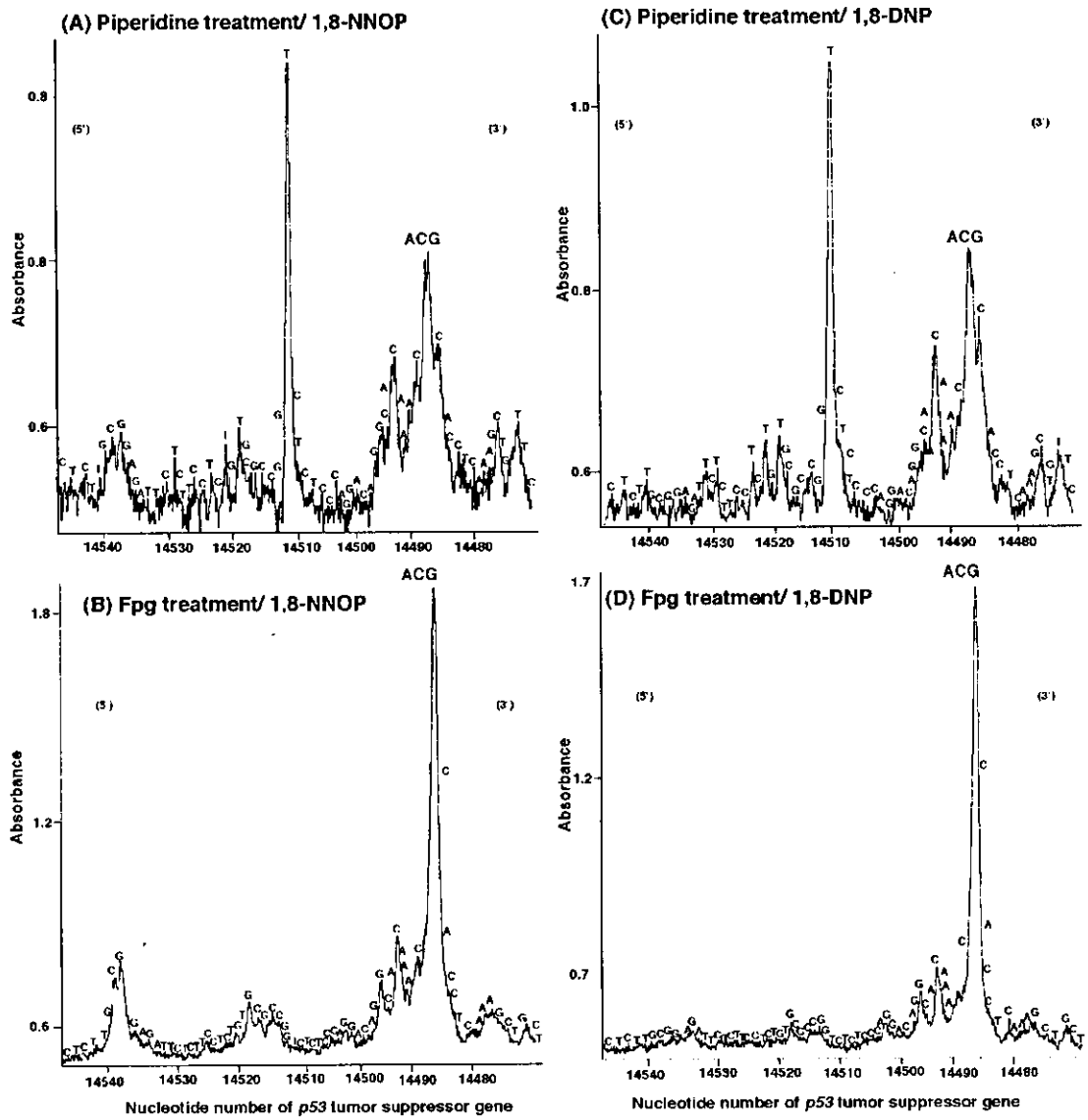

Figure 4. Site specificity of DNA cleavage induced by P450 reductase-treated 1,8-DNP and 1,8-NNOP in the presence of NADPH and Cu(II). The reaction mixtures containing 0.5 μM 1,8-NNOP (A, B) or 0.5 μM 1,8-DNP (C, D), 100 μM NADPH with (C, D) or without (A, B) 2.1 μg/mL P450 reductase were preincubated at 25 °C for 30 min in potassium phosphate buffer (pH 7.4). After preincubation, a ^{32}P-5′-end-labeled 443 bp DNA fragment, calf thymus DNA (20 μM/base), and 20 μM $CuCl_2$ were added to the mixtures. The reaction mixtures were incubated at 37 °C for 1 h, followed by piperidine treatment (A, C) or Fpg treatment (B, D). The horizontal axis shows the nucleotide number of the human *p53* tumor suppressor gene, and underscoring shows the complementary sequence to codon 273 (nucleotides 14486−14488).

(II) (data not shown). When P450 reductase was added, DNPs induced Cu(II)-mediated DNA damage (Figure 2A). 1,8-DNP and 1,6-DNP induced DNA damage more efficiently than 1,3-DNP did.

NNOPs, nitro-reduced metabolites of DNPs, were synthesized in order to compare with parent DNP. 1,8-NNOP and 1,6-NNOP induced DNA damage without P450 reductase (Figure 2B). These NNOPs induced DNA damage in the presence of NAD(P)H and Cu(II). In the absence of either NAD(P)H or Cu(II), NNOPs did not cause DNA damage. NNOPs alone did not cause DNA damage (data not shown).

Effects of Scavengers and Bathocuproine on DNA Damage. The effects of scavengers and bathocuproine on DNA damage by 1,8-DNP with P450 reductase are shown in Figure 3A. Mannitol and sodium formate, typical $^{\bullet}$OH scavengers, did not inhibit DNA damage. Catalase and bathocuproine, a Cu(I) specific chelator, inhibited DNA damage, whereas SOD did not reduce the amount of DNA damage. Similar inhibitory effects were observed in the cases of 1,8-NNOP (Figure 3B). When 1,6-isomers were used instead of 1,8-isomers, similar results were obtained (data not shown).

Site Specificity of DNA Damage by 1,8-DNP with P450 Reductase and 1,8-NNOP. An autoradiogram was scanned with a laser densitometer to measure the relative intensities of DNA cleavage products from the human *p53* tumor suppressor gene. 1,8-NNOP and P450 reductase-treated 1,8-DNP induced piperidine labile sites relatively at thymine and cytosine residues in the pres-

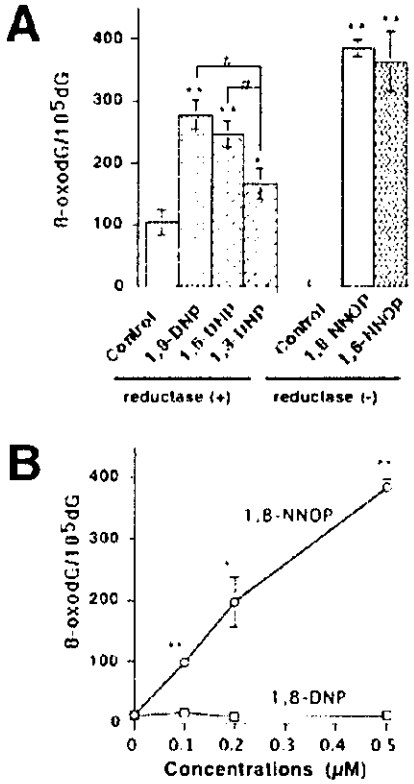

Figure 5. Formation of 8-oxodG by P450 reductase-treated DNPs and NNOPs in the presence of NADPH and Cu(II). For DNPs, the reaction mixtures containing 0.5 μM DNPs, 100 μM NADPH, and 2.1 μg/mL P450 reductase were preincubated at 25 °C for 30 min in potassium phosphate buffer (pH 7.4). After preincubation, calf thymus DNA (100 μM/base) and 20 μM $CuCl_2$ were added to the mixtures, followed by the incubation of 37 °C for 1 h. For NNOPs, the reaction mixtures containing calf thymus DNA (100 μM/base), 0.5 μM NNOPs (A), or the indicated concentrations of NNOPs (B), 100 μM NADPH, and 20 μM $CuCl_2$ were incubated at 37 °C for 1 h in potassium phosphate buffer (pH 7.4). After ethanol precipitation, DNA was enzymatically digested to individual nucleosides, and the 8-oxodG content was measured by HPLC-ECD as described in the Materials and Methods. Results are expressed as means and SD of values obtained from three independent experiments. Symbols indicate a significant difference as compared with control (*$P < 0.05$; **$P < 0.01$) and significant difference among DNPs (#$P < 0.05$) by *t*-test.

ence of Cu(II) and NAD(P)H (Figure 4A,C). With Fpg treatment, DNA cleavage occurred mainly at guanine and cytosine residues (Figure 4B,D). 1,8-NNOP and 1,8-DNP caused piperidine labile and Fpg sensitive lesions at CG in the 5′-ACG-3′ sequence, a well-known hotspot (*21*) of the *p53* gene.

Formation of 8-OxodG in Calf Thymus DNA. Using HPLC-ECD, we measured the 8-oxodG content of calf thymus DNA incubated with NNOPs and P450 reductase-treated DNPs (Figure 5A). P450 reductase-treated DNPs significantly increased the amount of 8-oxodG as compared with the control (1,8-DNP, $P < 0.01$; 1,6-DNP, $P < 0.01$; 1,3-DNP, $P < 0.05$). The order of 8-oxodG content was as follows: 1,8-DNP, 1,6-DNP > 1,3-DNP > control. 1,8-DNP and 1,6-DNP induced 8-oxodG formation more efficiently than 1,3-DNP ($P < 0.01$ and $P < 0.05$, respectively). There was no significant difference in 8-oxodG formation between 1,8-DNP and 1,6-DNP, after P450 reductase treatment. 1,8-NNOP and

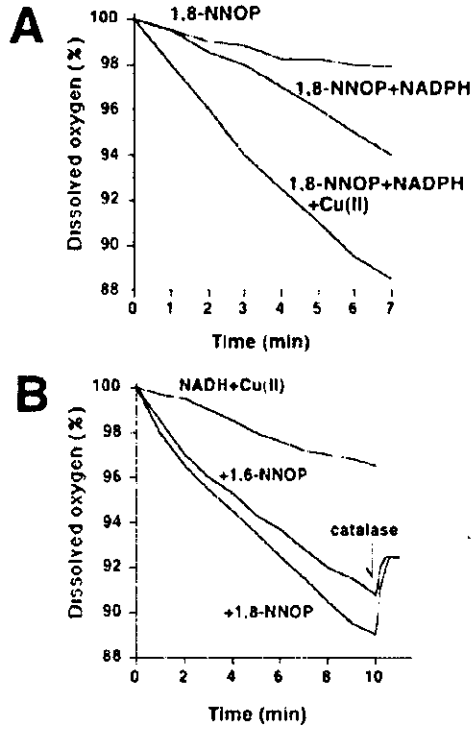

Figure 6. Oxygen consumption by the interaction of NNOPs with NAD(P)H and Cu(II). (A) Reaction mixtures contain 100 μM 1,8-NNOP, 2 mM NADPH, and/or 100 μM $CuCl_2$ in 2 mL of 10 mM phosphate buffer (pH 7.4) at 37 °C. (B) Reaction mixtures contain 100 μM NNOP, 2 mM NADH, and/or 100 μM $CuCl_2$ in 2 mL of 10 mM phosphate buffer (pH 7.8) at 37 °C. To detect H_2O_2 generation during oxygen consumption, 100 units of catalase were added at 10 min (indicated by an arrow).

1,6-NNOP without reductase significantly induced 8-oxodG formation in the presence of Cu(II) and NAD(P)H (Figure 5A).

1,8-NNOP significantly induced Cu(II)/NAD(P)H-mediated 8-oxodG formation in a dose-dependent manner (Figure 5B). 1,8-DNP induced no significant increase of 8-oxodG formation without P450 reductase. In the case of 1,6-NNOP, similar results were obtained (data not shown).

Oxygen Consumption during the Reaction of NNOP in the Presence of NADH and Cu(II). Oxygen consumption was observed in the reaction of 1,8-NNOP with NADH and Cu(II) (Figure 6). In the case of 1,8-NNOP alone, a little amount of oxygen consumption was observed. The addition of NADH increased oxygen consumption to some extent. In the reaction of 1,8-NNOP with NADH and Cu(II), a large amount of oxygen was consumed (Figure 6A). Figure 6B shows oxygen consumption by 1,8-NNOP and 1,6-NNOP in the presence of NADH and Cu(II). In the reaction of NADH and Cu(II), a little amount of oxygen consumption was observed. 1,8-NNOP induced oxygen consumption a little more efficiently than 1,6-NNOP. The addition of catalase increased dissolved oxygen, suggesting the generation of H_2O_2 that was decomposed by catalase to yield oxygen.

Discussion

The present study demonstrated the abilities of oxidative DNA damage by DNPs and their nitroso metabolites. NNOPs caused oxidative DNA damage in the presence

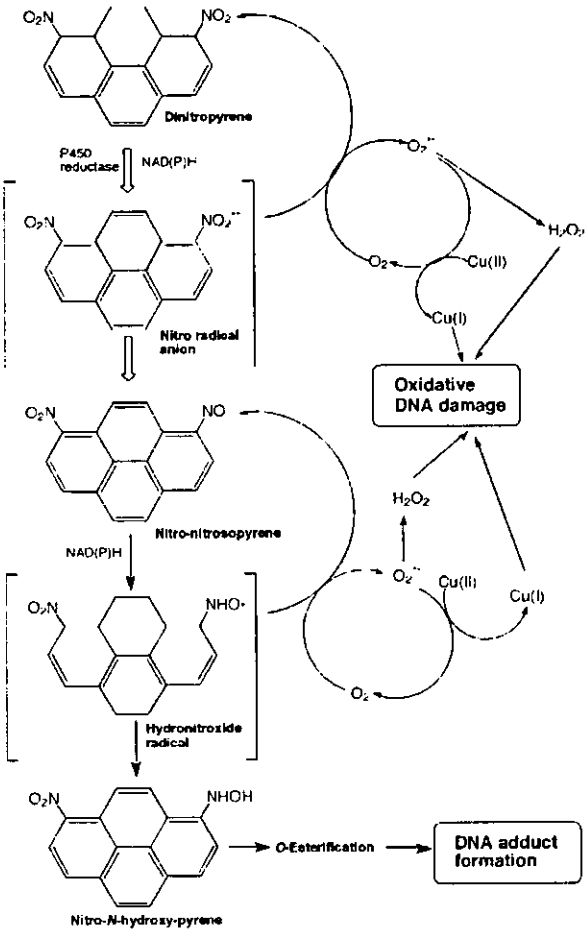

Figure 7. Proposed mechanism of oxidative DNA damage induced by DNPs in the presence of P450 reductase, NAD(P)H, and Cu(II).

of NAD(P)H and Cu(II), but DNPs did not. After the treatment of P450 reductase, DNPs, especially 1,8-DNP and 1,6-DNP, induced Cu(II)-mediated DNA damage. Both catalase and bathocuproine were found to reduce the DNA damage, indicating the involvement of H_2O_2 and Cu(I). These results suggested that NNOP was nonenzymatically reduced by NAD(P)H and autoxidized again by reacting with molecular oxygen to generate superoxide ($O_2^{\cdot-}$), and the addition of Cu(II) promoted the redox cycle. On the basis of these results, a possible mechanism could be proposed as follows (Figure 7). P450 reductase catalyzes one or more electron reduction of DNP to nitro radical anion and/or further reduced forms. Autoxidation of the reduced form yields $O_2^{\cdot-}$. NNOP can be reduced by an endogenous reductant NAD(P)H, to a reactive intermediate, which is probably a hydronitroxide radical. Autoxidation of this intermediate to NNOP occurs, coupled with the generation of $O_2^{\cdot-}$. $O_2^{\cdot-}$ is dismutated to H_2O_2 and reduces Cu(II) to Cu(I). H_2O_2, in turn, interacts with Cu(I) to form a reactive oxygen species, which causes DNA damage. Study using a Clarke oxygen electrode confirmed oxygen consumption by the reaction of NNOPs with NADH and Cu(II). The addition of catalase increased the level of dissolved oxygen by the decomposition of H_2O_2 to oxygen. It is suggested that the dissolved oxygen in the reaction mixture is converted to O_2 by the reduced forms of DNPs and NNOPs. Collectively, NNOP and P450 reductase-treated DNP significantly induce DNA damage including 8-oxodG formation through NAD(P)H-dependent redox cycles. The amounts of 8-oxodG induced by DNPs and NNOPs (0.5 μM) through the redox cycles corresponded to those induced by 30−60 μM H_2O_2 in the presence of Cu(II). The concentration of NAD(P)H in certain tissue has been estimated to be as high as 100−200 μM (*22*). The biological importance of NADH and NADPH as nuclear reductants (*23*) has been demonstrated before (*24*, *25*). P450 reductase and other enzymes with nitroreduction activity, such as NAD(P)H:quinone oxidoreductase and xanthine oxidase (*26*, *27*), may participate in activation of DNPs in vivo.

We showed that DNPs with P450 reductase treatment induced DNA damage including 8-oxodG formation in the intensity of 1,8-DNP, 1,6-DNP > 1,3-DNP. Consistently, among three DNP isomers, 1,3-DNP appears to be a weaker carcinogen (*1*) and mutagen (*3*, *4*). 1,6-DNP and 1,8-DNP are more efficiently nitro-reduced by liver cytosol and microsomes than 1,3-DNP (*28*). Similarly, Djuric (*29*) demonstrated that NADPH-mediated reduction of 1,3-NNOP to intermediates was slower than that of 1,6-NNOP. These differences in rates of enzyme efficacy to DNPs are considered to be one factor contributing to the differences of DNA damaging ability. This may explain the lower carcinogenic potential of 1,3-DNP as compared to 1,6-DNP and 1,8-DNP. Our results have suggested that DNPs are enzymatically reduced to NNOPs and are subsequently followed by the autoxidation of nitro radical anion and NAD(P)H-dependent reduction of NNOPs, resulting in Cu(II)-dependent redox cycle formation and DNA damage. This oxidative DNA damage may be supported by the report of Djuric et al. showing not only DNA adducts but also oxidative DNA damage in rats treated with 1,6-DNP (*8*).

Kohara et al. (*30*) showed that DNPs treatment increased the incidence of G · T transversions in mice. In this study, P450 reductase-treated DNPs induced Fpg sensitive sites preferentially at guanine residues and increased 8-oxodG formation. Shibutani et al. (*31*) have reported that 8-oxodG causes DNA misreplication, which can lead to mutation, particularly G · T substitutions. In addition, the bacterial mutation assay (*32*) revealed that DNPs exerted frequent base substitution mutations at cytosine residues. We demonstrated that NNOPs and P450 reductase-treated DNPs induced DNA cleavage sites preferentially at cytosine residues. Furthermore, piperidine and Fpg treatment detected cytosine and guanine damage of the ACG sequence complementary to codon 273, a well-known hotspot (*21*) of the *p53* gene. The occurrence of mutational hotspots may be partly explained by our observations. It is concluded that oxidative DNA damage, in addition to DNA adduct formation, may play important roles in the carcinogenesis of DNPs via metabolic activation on nitro group.

Acknowledgment. This work was supported by Grants-in-Aid for Scientific Research from the Ministry of Education, Science, Sports and Culture of Japan.

References

(1) IARC (1989) Diesel and gasoline engine exhausts and some nitroarenes. *IARC Monographs on the Evaluation of the Carcinogenic Risks to Humans*, Vol. 46, pp 1−373, IARC Press, Lyon.

(2) Watanabe, T., Hasei, T., Takahashi, Y., Otake, S., Murahashi, T., Takamura, T., Hirayama, T., and Wakabayashi, K. (2003) Mutagenic activity and quantification of nitroarenes in surface soil in the Kinki region of Japan. *Mutat. Res. 538*, 121−131.

(3) Busby, W. F., Jr., Penman, B. W., and Crespi, C. L. (1994) Human cell mutagenicity of mono- and dinitropyrenes in metabolically competent MCL-5 cells. *Mutat Res. 322*, 233−242.
(4) Busby, W. F., Jr., Smith, H., Bishop, W. W., and Thilly, W. G. (1994) Mutagenicity of mono- and dinitropyrenes in the *Salmonella typhimurium* TM677 forward mutation assay. *Mutat. Res. 322*, 221−232.
(5) Steenland, K., Deddens, J., and Stayner, L. (1998) Diesel exhaust and lung cancer in the trucking industry: Exposure-response analyses and risk assessment. *Am. J. Ind. Med. 34*, 220−228.
(6) Carroll, C. C., Warnakulasuriyarachchi, D., Nokhbeh, M. R., and Lambert, I. B. (2002) *Salmonella typhimurium* mutagenicity tester strains that overexpress oxygen-insensitive nitroreductases nfsA and nfsB. *Mutat. Res. 501*, 79−98.
(7) Hilario, P., Yan, S., Hingerty, B. E., Broyde, S., and Basu, A. K. (2002) Comparative mutagenesis of the C8-guanine adducts of 1-nitropyrene and 1,6- and 1,8-dinitropyrene in a CpG repeat sequence. A slipped frameshift intermediate model for dinucleotide deletion. *J. Biol. Chem. 277*, 45068−45074.
(8) Djuric, Z., Potter, D. W., Culp, S. J., Luongo, D. A., and Beland, F. A. (1993) Formation of DNA adducts and oxidative DNA damage in rats treated with 1,6-dinitropyrene. *Cancer Lett. 71*, 51−56.
(9) Ohnishi, S., Murata, M., Fukuhara, K., Miyata, N., and Kawanishi, S. (2001) Oxidative DNA damage by a metabolite of carcinogenic 1-nitropyrene. *Biochem. Biophys. Res. Commun. 280*, 48−52.
(10) Heflich, R. H., Fifer, E. K., Djuric, Z., and Beland, F. A. (1985) DNA adduct formation and mutation induction by nitropyrenes in Salmonella and Chinese hamster ovary cells: Relationships with nitroreduction and acetylation. *Environ. Health Perspect. 62*, 135−143.
(11) Fifer, E. K., Heflich, R. H., Djuric, Z., Howard, P. C., and Beland, F. A. (1986) Synthesis and mutagenicity of 1-nitro-6-nitrosopyrene and 1-nitro-8-nitrosopyrene, potential intermediates in the metabolic activation of 1,6- and 1,8-dinitropyrene. *Carcinogenesis 7*, 65−70.
(12) Chumakov, P. (1990) EMBL Data Library. Accession Number 54156.
(13) Serrano, M., Hannon, G. J., and Beach, D. (1993) A new regulatory motif in cell-cycle control causing specific inhibition of cyclin D/CDK4. *Nature 366*, 704−707.
(14) Capon, D. J., Chen, E. Y., Levinson, A. D., Seeburg, P. H., and Goeddel, D. V. (1983) Complete nucleotide sequences of the T24 human bladder carcinoma oncogene and its normal homologue. *Nature 302*, 33−37.
(15) Yamashita, N., Murata, M., Inoue, S., Hiraku, Y., Yoshinaga, T., and Kawanishi, S. (1998) Superoxide formation and DNA damage induced by a fragrant furanone in the presence of copper(II). *Mutat. Res. 397*, 191−201.
(16) Oikawa, S., Hirosawa, I., Hirakawa, K., and Kawanishi, S. (2001) Site specificity and mechanism of oxidative DNA damage induced by carcinogenic catechol. *Carcinogenesis 22*, 1239−1245.
(17) Yamamoto, K., and Kawanishi, S. (1989) Hydroxyl free radical is not the main active species in site-specific DNA damage induced by copper (II) ion and hydrogen peroxide. *J. Biol. Chem. 264*, 15435−15440.
(18) Murata, M., Mizutani, M., Oikawa, S., Hiraku, Y., and Kawanishi, S. (2003) Oxidative DNA damage by hyperglycemia-related aldehydes and its marked enhancement by hydrogen peroxide. *FEBS Lett. 554*, 138−142.
(19) Maxam, A. M., and Gilbert, W. (1980) Sequencing end-labeled DNA with base-specific chemical cleavages. *Methods Enzymol. 65*, 499−560.
(20) Ito, K., Inoue, S., Yamamoto, K., and Kawanishi, S. (1993) 8-Hydroxydeoxyguanosine formation at the 5′ site of 5′-GG-3′ sequences in double-stranded DNA by UV radiation with riboflavin. *J. Biol. Chem. 268*, 13221−13227.
(21) Levine, A. J., Momand, J., and Finlay, C. A. (1991) The p53 tumour suppressor gene. *Nature 351*, 453−456.
(22) Malaisse, W. J., Hutton, J. C., Kawazu, S., Herchuelz, A., Valverde, I., and Sener, A. (1979) The stimulus-secretion coupling of glucose-induced insulin release. XXXV. The links between metabolic and cationic events. *Diabetologia 16*, 331−341.
(23) Kukielka, E., and Cederbaum, A. I. (1994) Ferritin stimulation of hydroxyl radical production by rat liver nuclei. *Arch. Biochem. Biophys. 308*, 70−77.
(24) Ohnishi, S., Murata, M., and Kawanishi, S. (2002) Oxidative DNA damage induced by a metabolite of 2-naphthylamine, a smoking-related bladder carcinogen. *Jpn. J. Cancer Res. 93*, 736−743.
(25) Kawanishi, S., Hiraku, Y., Murata, M., and Oikawa, S. (2002) The role of metals in site-specific DNA damage with reference to carcinogenesis. *Free Radical Biol. Med. 32*, 822−832.
(26) Stiborova, M., Frei, E., Sopko, B., Sopkova, K., Markova, V., Lankova, M., Kumstyrova, T., Wiessler, M., and Schmeiser, H. H. (2003) Human cytosolic enzymes involved in the metabolic activation of carcinogenic aristolochic acid: Evidence for reductive activation by human NADPH: quinone oxidoreductase. *Carcinogenesis 24*, 1695−1703.
(27) Ritter, C. L., and Malejka-Giganti, D. (1998) Nitroreduction of nitrated and C-9 oxidized fluorenes in vitro. *Chem. Res. Toxicol. 11*, 1361−1367.
(28) Djuric, Z., Potter, D. W., Heflich, R. H., and Beland, F. A. (1986) Aerobic and anaerobic reduction of nitrated pyrenes in vitro. *Chem.-Biol. Interact. 59*, 309−324.
(29) Djuric, Z. (1992) Comparative reduction of 1-nitro-3-nitrosopyrene and 1-nitro-6-nitrosopyrene: Implications for the tumorigenicity of dinitropyrenes. *Cancer Lett. 65*, 73−78.
(30) Kohara, A., Suzuki, T., Honma, M., Oomori, T., Ohwada, T., and Hayashi, M. (2002) Dinitropyrenes induce gene mutations in multiple organs of the lambda/lacZ transgenic mouse (Muta Mouse). *Mutat. Res. 515*, 73−83.
(31) Shibutani, S., Takeshita, M., and Grollman, A. P. (1991) Insertion of specific bases during DNA synthesis past the oxidation-damaged base 8-oxodG. *Nature 349*, 431−434.
(32) Watanabe, T., Takashima, M., Kasai, T., and Hirayama, T. (1997) Comparison of the mutational specificity induced by environmental genotoxin nitrated polycyclic aromatic hydrocarbons in *Salmonella typhimurium* his genes. *Mutat. Res. 394*, 103−112.

TX0497550

A Planar Catechin Analogue Having a More Negative Oxidation Potential than (+)-Catechin as an Electron Transfer Antioxidant against a Peroxyl Radical

Ikuo Nakanishi,[†,‡] Kei Ohkubo,[†] Kentaro Miyazaki,[§,∥] Wataru Hakamata,[§] Shiro Urano,[∥] Toshihiko Ozawa,[†] Haruhiro Okuda,[§] Shunichi Fukuzumi,*[,‡] Nobuo Ikota,*[,‡] and Kiyoshi Fukuhara*[,§]

Redox Regulation Research Group, Research Center for Radiation Safety, National Institute of Radiological Sciences, Inage ku, Chiba 263 8555, Japan, Department of Material and Life Science, Graduate School of Engineering, Osaka University, CREST, Japan Science and Technology Agency, Suita, Osaka 565 0871, Japan, Division of Organic Chemistry, National Institute of Health Sciences, Setagaya ku, Tokyo 158 8501, Japan, and Department of Applied Chemistry, Shibaura Institute of Technology, Minato ku, Tokyo 108 8548, Japan

Received June 30, 2003

The hydrogen transfer reaction of antioxidative polyphenol with reactive oxygen species has proved to be the main mechanism for radical scavenging. The planar catechin (**P1H$_2$**), in which the catechol and chroman structure in (+) catechin (**1H$_2$**) are constrained to be planar, undergoes efficient hydrogen atom transfer toward galvinoxyl radical, showing an enhanced protective effect against the oxidative DNA damage induced by the Fenton reaction. The present studies were undertaken to further characterize the radical scavenging ability of **P1H$_2$** in the reaction with cumylperoxyl radical, which is a model radical of lipid peroxyl radical for lipid peroxidation. The kinetics of hydrogen transfer from catechins to cumylperoxyl radical has been examined in propionitrile at low temperature with use of ESR, showing that the rate of hydrogen transfer from **P1H$_2$** is significantly faster than that from **1H$_2$**. The rate was also accelerated by the presence of Sc(OSO$_2$CF$_3$)$_3$. Such an acceleration effect of metal ion indicates that the hydrogen transfer reaction proceeds via metal ion promoted electron transfer from **P1H$_2$** to oxyl radical followed by proton transfer rather than via a one step hydrogen atom transfer. The electrochemical ease of **P1H$_2$** for the one electron oxidation investigated by second harmonic alternating current voltammetry strongly supports the two step mechanism for hydrogen transfer, resulting in the enhanced radical scavenging ability.

Introduction

Recently, much attention has been directed to the possibility of natural antioxidants, such as flavonoids, vitamin C, vitamin E, and β carotene, as chemopreventive agents against oxdative stress and associated diseases (*1*−*3*). The generation of free radicals, such as hydroxyl radical (•OH) and superoxide anion ($O_2^{\bullet-}$), in biological systems is regarded as an important event contributing to the oxidative stress phenomena and one associated with many diseases, e.g., inflammentation, heart disease, cancer, and Alzheimer's (*4*−*6*). Flavonoids are plant phenolic compounds, which are widely distributed in foods and beverages and are extensively studied for their antioxidative and cytoprotective properties in various biological models (*7*−*9*). The antioxidative effects of flavonoids are believed to come from their inhibition of free radical processes in cells at three different levels: an initiation, by scavenging of $O_2^{\bullet-}$ (*10*, *11*); lipid peroxidation, by reaction with peroxyl or lipid peroxyl radicals (*12*); and the formation of •OH, probably by chelating iron ions (*13*). Besides their beneficial effects, there is also considerable evidence that flavonoids themselves are mutagenic (*14*, *15*) or carcinogenic (*16*) and show DNA damaging activity (*17*, *18*). Quercetin is a typical flavonoid that has been investigated as a potential chemopreventive agent against certain carcinogens (*19*, *20*). The chemistry of quercetin is predictive of its free radical scavenging ability. However, in biological systems, it was clearly demonstrated that quercetin could behave as both antioxidant and prooxidant. That is, dietary administration of excess quercetin induced renal tubule adenomas and adenocarcinomas in male rats (*21*) and induced intestinal and bladder cancer in rats (*22*). As other polyphenolic compounds, flavonoids may not show the sufficient antioxidative effects into the cells because of their hydrophilic properties, which impede the cell membrane translocation step (*23*). Therefore, much consideration to the safety should be required, when a large quantity of flavonoid is used as medicine for cancer chemoprevention.

In addition to the studies of natural antioxidants used for cancer chemoprevention or nutrition supplements, development of novel antioxidants that show improved radical scavenging activities has attracted considerable interest to remove reactive oxygen species (ROS), such as $O_2^{\bullet-}$ and •OH (*24*). We have previously reported that a planar catechin derivative (**P1H$_2$**) (Figure 1), synthesized in the reaction of (+) catechin (**1H$_2$**) with acetone

* To whom correspondence should be addressed. Tel: 81 3 3700 1141. Fax: 81 3 3707 6950. E mail: fukuhara@nibs.go.jp.
† National Institute of Radiological Sciences.
‡ Osaka University, CREST, Japan Science and Technology Agency.
§ National Institute of Health Sciences.
∥ Shibaura Institute of Technology.

10.1021/tx034134c CCC: $27.50
Published on Web 12/03/2003

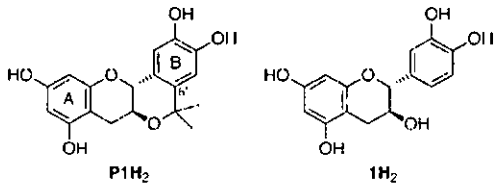

P1H$_2$ **1H$_2$**

Figure 1. Chemical structures of planar catechin (**P1H$_2$**) and (+) catechin (**1H$_2$**).

in the presence of BF_3·Et_2O (*25, 26*), shows an enhanced protective effect against the oxidative DNA damage induced by the Fenton reaction without the prooxidant effect, which is usually observed in the case of **1H$_2$**. The spectroscopic and kinetic studies have demonstrated that the rate of hydrogen transfer from **P1H$_2$** to galvinoxyl radical (G$^\bullet$), a stable oxygen centered radical, is about 5 fold faster than that of hydrogen transfer from the native **1H$_2$** to G$^\bullet$ (*26*). We have also demonstrated that the $O_2^{\bullet-}$ generating ability of the dianion form of **P1H$_2$** generated in the reaction of **P1H$_2$** with 2 equiv of Bu_4NOMe in deaerated acetonitrile (MeCN) is much lower than that of **1H$_2$**, suggesting that **P1H$_2$** may be a promising novel antioxidant with reduced prooxidant activity (*27*). In addition, as compared with the hydrophilic **1H$_2$**, the lipophilic property of **P1H$_2$**, which is very soluble in alcohol, ether, and tetrahydrofuran, seems to give rise to its antioxidative activity into cell membrane.

We report herein that **P1H$_2$** can also scavenge cumyl peroxyl radical (PhCMe$_2$OO$^\bullet$) more efficiently than **1H$_2$**. PhCMe$_2$OO$^\bullet$, while much less reactive than alkoxyl radicals, is known to follow the same pattern of relative reactivity with a variety of substrates (*28*–*30*). The effect of a metal ion on the rate of hydrogen transfer from **P1H$_2$** to PhCMe$_2$OO$^\bullet$ was also examined in order to distinguish between the one step hydrogen atom transfer and the electron transfer mechanisms in the radical scavenging reaction of **P1H$_2$** (*31*). The one electron oxidation potential (E_{ox}^{1}) of **1H$_2$** as well as that of **P1H$_2$** in MeCN was determined by the second harmonic alternating current voltammetry (SHACV). The combination of kinetic and electrochemical results obtained in this study provides confirmative bases to develop novel antioxidants that show improved radical scavenging activities.

Materials and Methods

Materials. A planar catechin derivative (**P1H$_2$**) was synthesized according to the literature procedure (*26*). (+) Catechin (**1H$_2$**) was purchased from Sigma. Di *tert* butyl peroxide was obtained from Nacalai Tesque Co., Ltd., and purified by chromatography through alumina, which removes traces of the hydroperoxide. Cumene was purchased from Wako Pure Chemical Industries Ltd., Japan. Tetra *n* butylammonium perchlorate (TBAP) used as a supporting electrolyte was recrystallized from ethanol and dried under vacuum at 313 K. MeCN and propionitrile (EtCN) used as solvent were purified and dried by the standard procedure (*32*).

Spectral and Kinetic Measurements. Kinetic measurements for the hydrogen transfer reactions between catechins and cumylperoxyl radical were performed on a JEOL X band spectrometer (JES ME LX) at 203 K. Typically, photoirradiation of an oxygen saturated EtCN solution containing di *tert* butyl peroxide (1.0 M) and cumene (1.0 M) with a 1000 W high pressure Mercury lamp resulted in formation of cumylperoxyl radical (PhCMe$_2$OO$^\bullet$: g = 2.0156), which could be detected at low temperatures. The g values were calibrated by using an Mn^{2+} marker. Upon cutting off the light, the decay of the ESR intensity was recorded with time. The decay rate was accelerated by the presence of **P1H$_2$** (1.0×10^{-4} M). Rates of hydrogen transfer from **P1H$_2$** to PhCMe$_2$OO$^\bullet$ were monitored by measuring the decay of the ESR signal of PhCMe$_2$OO$^\bullet$ in the presence of various concentrations of **P1H$_2$** in EtCN at 203 K. Pseudo first order rate constants were determined by a least squares curve fit using an Apple Macintosh personal computer. The first order plots of $\ln(I - I_\infty)$ vs time (I and I_∞ are the ESR intensity at time t and the final intensity, respectively) were linear for three or more half lives with the correlation coefficient, $\rho > 0.99$. In each case, it was confirmed that the rate constants derived from at least five independent measurements agreed within an experimental error of 15%.

Scheme 1

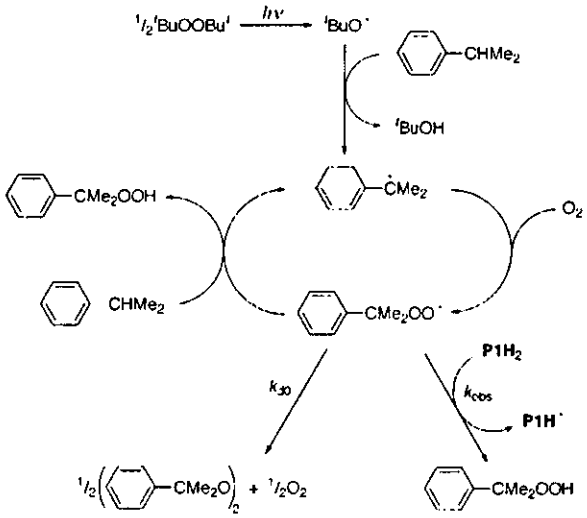

Electrochemical Measurements. The SHACV (*33*–*38*) measurements of **1H$_2$** and **P1H$_2$** were performed on an ALS 630A electrochemical analyzer in deaerated MeCN containing 0.10 M TBAP as a supporting electrolyte at 298 K. The platinum working electrode was polished with BAS polishing alumina suspension and rinsed with acetone before use. The counter electrode was platinum wire. The measured potentials were recorded with respect to an Ag/$AgNO_3$ (0.01 M) reference electrode. The one electron oxidation potentials (E_{ox}^{1}) (vs Ag/$AgNO_3$) were converted into those vs SCE by addition of 0.29 V (*39*).

Results

Hydrogen Transfer from Catechins to Cumylperoxyl Radical. Direct measurements of the rates of hydrogen transfer from a planar catechin derivative (**P1H$_2$**) to cumylperoxyl radical were performed in EtCN at 203 K by means of ESR. The photoirradiation of an oxygen saturated EtCN solution containing di *tert* butylperoxide (Bu^{t}OOBu^t) and cumene with a 1000 W high pressure mercury lamp results in formation of cumyl peroxyl radical (PhCMe$_2$OO$^\bullet$), which was readily detected by ESR. The cumylperoxyl radical is formed via a radical chain process shown in Scheme 1 (*40*–*44*).

The photoirradiation of Bu^{t}OOBu^t results in the homolytic cleavage of the O–O bond to produce Bu^{t}O$^\bullet$ (*45*–*51*), which abstracts a hydrogen from cumene to give cumyl radical, followed by the facile addition of oxygen to cumyl radical. The cumylperoxyl radical can also abstract a hydrogen atom from cumene in the propagation step to yield cumene hydroperoxide, accompanied by regeneration of cumyl radical (Scheme 1) (*52, 53*). In the termination step, cumylperoxyl radicals decay by a bimolecular reaction to yield the corresponding peroxide

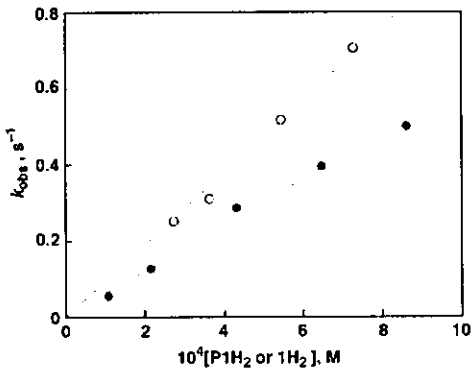

Figure 2. Plots of k_{obs} vs **P1H$_2$** (white circles) and vs **1H$_2$** (black circles) for the reactions of catechins (**P1H$_2$** and **1H$_2$**) with cumylperoxyl radical in EtCN at 203 K.

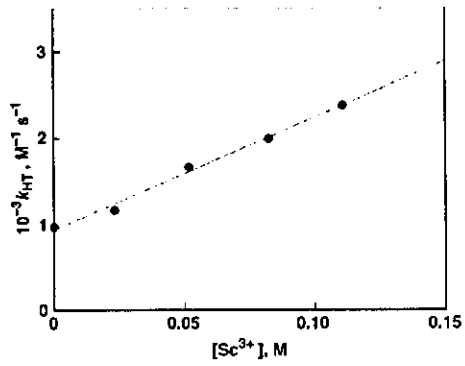

Figure 3. Plot of k_{HT} vs [Sc^{3+}] in the reaction of **P1H$_2$** to cumylperoxyl radical in the presence of $Sc(OSO_2CF_3)_3$ in EtCN at 203 K.

and oxygen (Scheme 1) (*41, 42*). When the light is cut off, the ESR signal intensity decays obeying second order kinetics due to the bimolecular reaction in Scheme 1.

In the presence of **P1H$_2$**, however, the decay rate of cumylperoxyl radical after cutting off the light becomes much faster than that in the absence of **P1H$_2$**. The decay rate in the presence of **P1H$_2$** (1.0×10^{-4} M) obeys pseudo first order kinetics. This decay process is ascribed to hydrogen transfer from **P1H$_2$** to cumylperoxyl radical (Scheme 1). The pseudo first order rate constants increase with increasing **P1H$_2$** concentration ([**P1H$_2$**]) to exhibit first order dependence on [**P1H$_2$**] as shown in Figure 2. From the slope of the linear plot of k_{obs} vs concentration of **P1H$_2$** is determined the second order rate constant (k_{HT}) for the hydrogen transfer from **P1H$_2$** to cumylperoxyl radical as 9.7×10^2 M^{-1} s^{-1} in EtCN at 203 K.

Figure 2 also shows the linear plot of k_{obs} vs the concentration of (+) catechin (**1H$_2$**) for the reaction of **1H$_2$** with cumylperoxyl radical in EtCN at 203 K. The k_{HT} value for **1H$_2$** was also determined in the same manner as 6.0×10^2 M^{-1} s^{-1} (*31*). Thus, as in the case of galvinoxyl radical (*26*), the hydrogen transfer rate from **P1H$_2$** to cumylperoxyl radical is significantly faster than that from **1H$_2$**.

We have recently reported that the hydrogen transfer from **1H$_2$** to galvinoxyl or cumylperoxyl radical proceeds via electron transfer from **1H$_2$** to galvinoxyl or cumylperoxyl radical, which is accelerated by the presence of metal ions, such as Mg^{2+} and Sc^{3+}, followed by proton transfer (*31*). In such a case, the coordination of the metal ion to the one electron reduced species of galvinoxyl or cumylperoxyl radical may stabilize the product, resulting in acceleration of the electron transfer process. In this context, the effect of a metal ion on the k_{HT} value of **P1H$_2$** was examined. As in the case of **1H$_2$**, the hydrogen transfer from **P1H$_2$** to cumylperoxyl radical was significantly accelerated by the presence of $Sc(OSO_2CF_3)_3$ as shown in Figure 3. Thus, the hydrogen transfer from **P1H$_2$** to cumylperoxyl radical also proceeded via electron transfer from **P1H$_2$** to cumylperoxyl radical followed by proton transfer from **P1H$_2$**$^{\bullet+}$ to one electron reduced species cumylperoxyl radical as shown in Scheme 2.

The larger k_{HT} value of **P1H$_2$** as compared to that of **1H$_2$** may be ascribed to the stability of the radical cation of **P1H$_2$** (**P1H$_2$**$^{\bullet+}$), which is produced in the electron transfer from **P1H$_2$** to cumylperoxyl radical. The electron donating *i*propyl group at the B ring of **P1H$_2$** may

Scheme 2

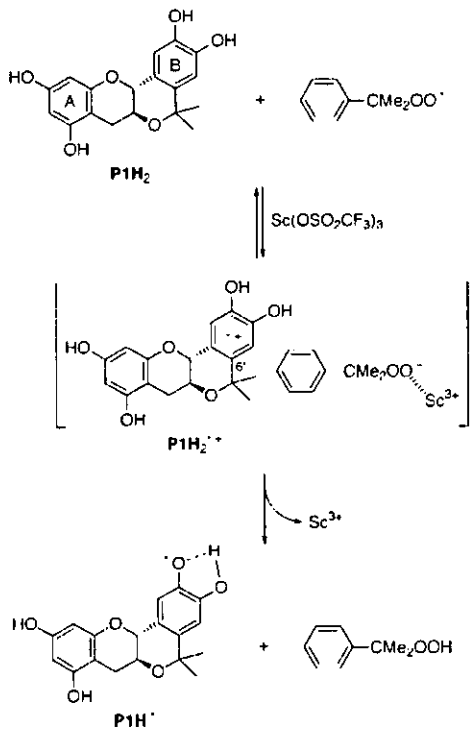

significantly stabilize **P1H$_2$**$^{\bullet+}$, resulting in the acceleration of the electron transfer step. In such a case, the one electron oxidation potential of **P1H$_2$** is expected to be more negative than that of **1H$_2$**.

One-Electron Oxidation Potential of a Planar Catechin Analogue. To determine the one electron oxidation potential of **P1H$_2$**, the cyclic voltammogram of **P1H$_2$** was recorded in MeCN containing 0.1 M TBAP as a supporting electrolyte at 298 K. Two irreversible oxidation (anodic) peaks were observed at 1.22 and 1.41 V vs SCE (data not shown). A similar cyclic voltammogram was obtained for **1H$_2$**, which exhibits irreversible oxidation peaks at 1.16 and 1.35 V vs SCE. This indicates that radical cations of **P1H$_2$** and **1H$_2$** are too unstable at the time scale of CV measurements. The SHACV method is known to provide a superior approach to directly evaluating one electron redox potential in the presence of the follow up chemical reaction relative to the better known dc and fundamental harmonic ac method (*34*). The

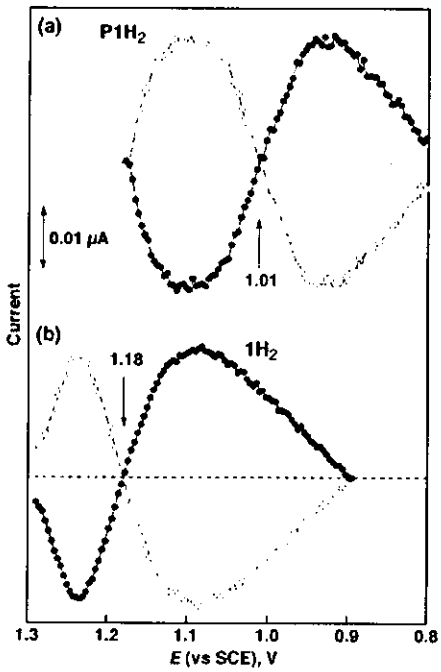

Figure 4. SHACVs of (a) $\mathbf{P1H_2}$ and (b) $\mathbf{1H_2}$ in deaerated MeCN containing 0.1 M TBAP at 298 K. Scan rate, 4 mV s^{-1}; working electrode, Pt.

SHACV method was applied to determine the one-electron oxidation potentials (E_{ox}^0) of $\mathbf{P1H_2}$ and $\mathbf{1H_2}$ in deaerated MeCN containing 0.1 M TBAP at 298 K. Figure 4 shows the SHACV of $\mathbf{P1H_2}$ and $\mathbf{1H_2}$. The E_{ox}^0 value of $\mathbf{P1H_2}$ thus determined (1.01 V vs SCE) is significantly more negative than that of $\mathbf{1H_2}$ (1.18 V vs SCE) as expected above. Thus, $\mathbf{P1H_2}$ may undergo one electron oxidation by cumylperoxyl radical more easily than $\mathbf{1H_2}$, showing excellent radical scavenging abilities.

Discussion

The primary goal of this project is to develop a novel antioxidant, which can be positively utilized for clinical treatment and/or chemoprevention of diseases associated with ROS. There are two kinds of strategy in considering the development of synthetic antioxidants: one is a design of a new type of antioxidant, the structure of which is different from the natural antioxidant, and the other is a modification of natural antioxidants to improve its antioxidative capacities. A recent topic on the synthetic antioxidants is a development and clinical application of edaravone (3 methyl 1 phenyl 2 pyrazolin 5 one, MCI 186). Edaravone has been reported to show potent free radical scavenging actions toward ROS, such as $O_2^{\bullet-}$, H_2O_2, and HClO, which may be involved in the tissue destructive effects of reperfusion after ischemia (*54*−*56*). As a neuroprotective agent, edaravone has been clinically prescribed in Japan since 2001 to treat patients with cerebral ischemia. Regarding flavonoids, there are many reports for the synthetic derivatives to exert prominent chemopreventive effects toward oxidative stress derived injury. However, only a few studies on the synthetic flavonoids, which were aimed at the improved radical scavenging ability, have been reported. Flavopiridol is a chlorinated derivative of flavone, which is currently in clinical development for the treatment of advanced cancer, including ovarian cancer (*57*, *58*). Flavopiridol is an inhibitor of cycline dependent kinases to modulate cell cycle (*59*), and radical scavenging mechanism is not involved in the expression of anticancer effects of this compound.

The planar catechin ($\mathbf{P1H_2}$), which has been detected in mere trace amounts in nature (*60*), is easily synthesized by the reaction of $\mathbf{1H_2}$ and acetone (*26*). The ability of $\mathbf{P1H_2}$ to scavenge oxygen centered radical, such as galvinoxyl radical, is excellent as compared to that of (+) catechin and its complete inhibition of oxidative DNA damage induced by metal catalyzed generation of hydroxyl radical (*26*), as well. Therefore, $\mathbf{P1H_2}$ may exert its antioxidative capacities by scavenging reactive oxygen radicals in many types of biologically generating systems. The present study was focused on the reaction of $\mathbf{P1H_2}$ to cumylperoxyl radical, a model radical of lipid peroxyl radical formed in a radical chain reaction of lipid peroxidation. The processes of lipid peroxidation concomitant with the formation of lipid peroxyl radicals are detrimental to the viability of the cell. The biophysical consequences of peroxidation on membrane phospholipids can be both extensive and highly destructive, provoking diseased states such as atherosclerosis, heart attacks, cancer, ischaemia/repulsion injury, and even the aging process as a whole (*61*). The ability of antioxidant to scavenge peroxyl radicals and block lipid peroxidation raises the possibility that it may protect against the many types of free radical associated diseases. As compared with $\mathbf{1H_2}$, $\mathbf{P1H_2}$ showed strong radical scavenging ability toward cumylperoxyl radical formed via a radical chain process, as well as the predominant radical scavenging reaction of $\mathbf{P1H_2}$ to galvinoxyl radical. Lipid peroxyl radical formed by the reaction between a lipid radical and a molecular oxygen is essential for autoxidation of lipid. The peroxyl radical abstracts an allylic hydrogen atom from an adjacent polyunsaturated fatty acid, resulting in a lipid hydroperoxide and a second lipid radical. Therefore, $\mathbf{P1H_2}$ may act as an effective terminator by means of scavenging free radicals in autoxidation of lipids.

Considering the antioxidative mechanism to scavenge peroxyl radical, there are two possibilities in the mechanism of hydrogen transfer reactions, i.e., a one step hydrogen atom transfer or electron transfer followed by proton transfer. The hydrogen transfer reaction from $\mathbf{P1H_2}$ to cumylperoxyl radical accelerated in the presence of the metal ion, indicating that the hydrogen transfer reaction proceeded by the two step reaction, that is, electron transfer from $\mathbf{P1H_2}$ to cumylperoxyl radical followed by proton transfer from $\mathbf{P1H_2}^{\bullet+}$. Vitamin E is a typical antioxidant to terminate lipid peroxidation, and the hydrogen transfer reaction proceeds via a one step hydrogen atom transfer process, which is due to no effect of metal ion on the hydrogen transfer rate from vitamin E analogue to galvinoxyl radical (*62*). On the other hand, in the case of $\mathbf{1H_2}$, the hydrogen transfer reaction proceeds via electron transfer from $\mathbf{1H_2}$ to oxyl radical followed by proton transfer rather than via a one step hydrogen atom transfer (*31*), as the case of present results of the $\mathbf{P1H_2}$. The one electron oxidation potential investigated by the SHACV indicated that the electrochemical oxidation of $\mathbf{P1H_2}$ was easier to progress in comparison with $\mathbf{1H_2}$. The electron transfer mechanism for the radical scavenging reaction of $\mathbf{P1H_2}$ is probably a consequence of its electrochemical ease for one electron oxidation. Judging from the one electron oxidation po

tential of $\mathbf{P1H_2}$ that is higher than the one electron reduction potential of cumylperoxyl radical ($E^0_{red} = 0.65$ V vs SCE) (*63*), the free energy changes of electron transfer from $\mathbf{P1H_2}$ to cumylperoxyl radical are positive [ΔG_{et}^0 (in eV) $= e(E^0_{ox} - E^0_{red}) > 0$, where e is elementary charge]; thereby, the electron transfer step is endergonic. In such a case, the initial electron transfer rate (k_{et}) may be the rate determining step in the overall rate of hydrogen transfer, which consists of electron and proton transfer steps. The maximum k_{et} value is evaluated from the ΔG_{et}^0 value by eq 1, where it is assumed that the activation free energy ($\Delta G_{et}^{\ddagger}$) is equal to ΔG_{et}^0 (no additional barrier is involved). Z is the frequency factor taken as 1×10^{11} M^{-1} s^{-1}, and k_B is the Boltzmann constant (*64, 65*).

$$k_{et} = Z \exp(-\Delta G_{et}^{\ddagger}/k_B T) \qquad (1)$$

The maximum k_{et} value is calculated as 1.2×10^2 M^{-1} s^{-1}, which is the same order of magnitude as the observed k_{HT} value (9.0×10^2 M^{-1} s^{-1}). The larger k_{HT} value than the k_{et} value indicates that the hydrogen transfer from $\mathbf{P1H_2}$ to cumylperoxyl radical proceeds via a rate determining electron transfer with an interaction between $\mathbf{P1H_2}$ and cumylperoxyl radical. The formation of charge transfer complexes between cumylperoxyl radical and a variety of electron acceptors has been well documented in the literature (*66, 67*). Thus, the hydrogen transfer may proceed via an inner sphere electron transfer in the charge transfer complex formed between $\mathbf{P1H_2}$ and cumylperoxyl radical. The acceleration of the hydrogen transfer rate in the presence of Sc^{3+} (Figure 3) is ascribed to the promoting effect of Sc^{3+} on the electron transfer step due to the strong binding of Sc^{3+} with cumylperoxyl anion produced in the electron transfer.

In conclusion, the hydrogen transfer from $\mathbf{P1H_2}$ to cumylperoxyl radical generated in radical chain reactions proceeds via an electron transfer reaction and the rate of hydrogen transfer from $\mathbf{P1H_2}$ to cumylperoxyl radical is faster than that from $\mathbf{1H_2}$. The predominance of $\mathbf{P1H_2}$ in the hydrogen transfer reaction is consistent with the electrochemical ease for its one electron oxidation potential. Since $\mathbf{P1H_2}$ is very lipophilic as compared to (+)-catechin itself, it is proposed that $\mathbf{P1H_2}$ interacts and penetrates the lipid bilayer giving rise to its maximized antioxidant capacity. Therefore, we believe that $\mathbf{P1H_2}$ may be significantly more effective not only for protecting tissue from the onslaught of the radical species governing peroxidation but also for terminating the autoxidation, which plays in provoking diseased states. Studies are underway to investigate basic biochemical properties of $\mathbf{P1H_2}$ in vivo, as well as to investigate its ability to serve as an antioxidant for the treatment of diseases associated with oxidative stress.

Acknowledgment. This work was partially supported by a Grant in Aid for Scientific Research Priority Area (No. 11228205) and a Grant in Aid for Young Scientist (B) (No. 15790032) from the Ministry of Education, Culture, Sports, Science and Technology, Japan, partly by a Grant (MF 16) from the Organization for Pharmaceutical Safety and Research, and by a Grant in Aid for the Scientific Research (No. 14141201) from the Ministry of Health Labor and Welfare.

References

(1) Marchioli, R. (1999) Antioxidant vitamins and prevention of cardiovascular disease: laboratory, epidemiological and clinical trial data. *Pharmacol. Res. 40*, 227−238.

(2) Colic, M., and Pavelic, K. (2000) Molecular mechanisms of anticancer activity of natural dietetic products. *J. Mol. Med. 78*, 333−336.

(3) Willis, M. S., and Wians, F. H. (2003) The role of nutrition in preventing prostate cancer: a review of the proposed mechanism of action of various dietary substances. *Clin. Chim. Acta 330*, 57−83.

(4) Jadhav, S. J., Nimbalkar, S. S., Kulkarni, A. D., and Madhavi, D. L. (1996) Lipid oxidation in biological and food systems. In *Food Antioxidants* (Madhavi, D. L., Deshpande, S. S., and Salunkhe, D. K., Eds.) pp 5−63, Deller, New York.

(5) Sies, H. (1987) *Oxidative Stress*, Academic Press, London.

(6) Katzman, R., and Kawas, C. (1994) The epidemiology of dementia and Alzheimer's disease. In *Alzheimer Disease* (Terry, R. D., Katzman, R., and Bick, K. L., Eds.) pp 103−119, Raven Press, New York.

(7) Cody, V., Middleton, E., and Harborne, J. B. (1986) *Plant Flavonoids in Biology and Medicine: Biochemical Pharmacological and Structure−Activity Relationships*, Alan R. Liss, New York.

(8) Middleton, E., Jr., and Kandaswami, C. (1993) The impact of plant flavonoids on mammalian biology: implications for immunity, inflammation and cancer. In *The Flavonoids: Advances in Research Since 1986* (Harborne, J. H., Ed.) pp 619−652, Chapman and Hall, New York.

(9) Rice-Evance, C. A., Miller, N. J., and Paganga, G. (1996) Structure−antioxidant activity relationships of flavonoids and phenolic acids. *Free Radical Biol. Med. 20*, 933−956.

(10) Jovanovic, S. V., Steenken, S., Tosic, M., Marjanovic, B., and Simic, M. G. (1994) Flavonoids as antioxidants. *J. Am. Chem. Soc. 116*, 4846−4851.

(11) Ho, J. P., Calomme, M., Lasure, A., De Bruyne, T., Pieters, L., Vlietinck, A., and Vanden Berghe, D. A. (1995) Structure−activity relationships of flavonoids with superoxide scavenging ability. *Biol. Trace Elem. Res. 47*, 327−331.

(12) Terao, J., Piskula, M., and Yao, Q. (1994) Protective effect of epicatechin, epicatechin gallate and quercetin on lipid peroxidation in phospholipids bilayers. *Arch. Biochem. Biophys. 308*, 278−284.

(13) Morel, J., Lescoat, G., Cogrel, P., Sergent, O., Pasdeloup, N., Brissot, P., Cillard, P., and Cillard, J. (1993) Antioxidant and iron chelating activities of the flavonoids catechin, quercetin and diosmetin on iron loads rat hepatocyte cultures. *Biochem. Pharmacol. 45*, 13−19.

(14) Sugimura, T., Nagao, M., Matsushima, T., Yahagi, T., Seino, Y., Shirai, A., Sawamura, M., Natori, S., Yoshihira, K., Fukuoka, M., and Kuroyanagi, M. (1977) Mutagenicity of flavone dericatives. *Proc. Jpn. Acad. B 53*, 194−197.

(15) Ochiai, M., Nagao, M., Wakabayashi, K., and Sugimura, T. (1984) Superoxide dismutase acts an enhancing factor for quercetin mutagenesis in rat liver cytosol by preventing its decomposition. *Mutat. Res. 129*, 19−24.

(16) Das, A., Wang, J. H., and Lien, E. J. (1994) Carcinogenicity, mutagenicity and cancer preventing activities of flavonoids: a structure system activity relationship (SSAR) analysis. *Prog. Drug Res. 42*, 133−166.

(17) Sahu, S. C., and Washington, M. C. (1991) Effects of antioxidants on quercetin induced nuclear DNA damage and lipid peroxidation. *Cancer Lett. 60*, 259−264.

(18) Duthie, S. J., Johnson, W., and Dobson, V. L. (1997) The effect of dietary flavonoids on DNA damage (strand breaks and oxidized pyrimidines) and growth in human cells. *Mutat. Res. 390*, 141−151.

(19) Verma, A. K., Johnson, J. A., Gould, M. N., and Tanner, M. A. (1988) Inhibition of 7,12-dimethylbenz[*a*]anthracene- and *N*-nitrosomethylurea-induced rat mammary cancer by dietary flavonol quercetin. *Cancer Res. 48*, 5754−5758.

(20) Deschner, E. E., Ruperto, J., Wong, G., and Newmark, H. L. (1991) Quercetin and rutin as inhibitors of azoxymethanol-induced colonic neoplasia. *Carcinogenesis 12*, 1193−1196.

(21) *Toxicology and Carcinogenesis Studies of Quercetin in F344 Rats* (1992) National Toxicology Program (NTP) Technical Report, NTP TR 409, NIH Publication No. 93-147478, National Institutes of Health, Bethesda, MD.

(22) Pamukcu, A. M., Yalciner, S., Hatcher, J. F., and Bryan, G. T. (1980) Quercetin, a rat intestinal and bladder carcinogen present in bracken fern (*Pteridium aquilinum*). *Cancer Res. 40*, 3468−3472.

(23) Kandaswami, C., Perkins, E., Soloniuk, D. S., Drzewiecki, G., and Middleton, E., Jr. (1991) Antiproliferative effects of citrus flavonoids on a human squamous cell carcinoma in vitro. *Cancer Lett. 56*, 147−152.

(24) Yoshikawa, T., Toyokuni, S., Yamamoto, Y., and Naito, Y. (2000) *Free Radical in Chemistry, Biology and Medicine*, OICA International (U.K.) Ltd., London.
(25) Guiso, M., Marra, C., and Cavarischia, C. (2001) Isochromans from 2 (3′,4′ dihydroxy)phenylethanol. *Tetrahedron Lett. 42*, 6531−6534.
(26) Fukuhara, K., Nakanishi, I., Kansui, H., Sugiyama, E., Kimura, M., Shimada, T., Urano, S., Yamaguchi, K., and Miyata, N. (2002) Enhanced radical scavenging activity of a planar catechin analogue. *J. Am. Chem. Soc. 124*, 5952−5953.
(27) Fukuhara, K., Nakanishi, I., Shimada, T., Ohkubo, K., Miyazaki, K., Hakamata, W., Urano, S., Ozawa, T., Okuda, H., Miyata, N., Ikota, N., and Fukuzumi, S. (2003) A planar catechin analogue as a promising antioxidant with reduced prooxidant activity. *Chem. Res. Toxicol. 16*, 81−86.
(28) Russel, G. A. (1973) Reactivity, selectivity, and polar effects in hydrogen atom transfer reactions. In *Free Radicals* (Kochi, J. K., Ed.) pp 275−331, John Wiley & Sons, New York.
(29) Russel, G. A. (1956) The rates of oxidation of aralkyl hydrocarbons. Polar effects in free radical reactions. *J. Am. Chem. Soc. 78*, 1047−1054.
(30) Howard, J. A., Ingold, U. K., and Symonds, M. (1968) Absolute rate constants for hydrocarbon oxidation VIII. Reactions of cumylperoxyl radicals. *Can. J. Chem. 46*, 1017−1022.
(31) Nakanishi, I., Miyazaki, K., Shimada, T., Ohkubo, K., Urano, S., Ikota, N., Ozawa, T., Fukuzumi, S., and Fukuhara, K. (2002) Effects of metal ions distinguishing between one step hydrogen and electron transfer mechanisms for the radical scavenging reaction of (+) catechin. *J. Phys. Chem. A 106*, 11123−11126.
(32) Perrin, D. D., Armarego, W. L. F., and Perrin, D. R. (1988) *Purification of Laboratory Chemicals*, Pergamon Press, Elmsford, New York.
(33) McCord, T. G., and Smith, D. E. (1969) Second harmonic a.c. polarography. Theoretical predictions for systems with first order chemical reactions following the charge transfer step. *Anal. Chem. 41*, 1423−1441.
(34) Bond, A. M., and Smith, D. E. (1974) Direct measurement of $E^0_{1/2}$ with reversible EC electrode processes by second harmonic alternating current polarography and voltammetry. *Anal. Chem. 46*, 1946−1951.
(35) Wasielewski, M. R., and Breslow, R. (1976) Thermodynamic measurements on unsubstituted cyclopropenyl radical and anion, and derivatives by second harmonic alternating current voltammetry of cyclopropenyl cations. *J. Am. Chem. Soc. 98*, 4222−4229.
(36) Arnett, E. M., Amarnath, K., Harvey, N. G., and Cheng, J. P. (1990) Determination and interrelation of bond heterolysis and homolysis energies in solution. *J. Am. Chem. Soc. 112*, 344−355.
(37) Patz, M., Mayr, H., Maruta, J., and Fukuzumi, S. (1995) Reactions of carbocations with π nucleophiles: polar mechanism and no outer sphere electron transfer processes. *Angew. Chem., Int. Ed. Engl. 34*, 1225−1227.
(38) Fukuzumi, S., Satoh, N., Okamoto, T., Yasui, K., Suenobu, T., Seko Y., Fujitsuka, M., and Ito, O. (2001) Change in spin state and enhancement of redox reactivity of photoexcited states of aromatic carbonyl compounds by complexation with metal ion salts acting as Lewis acids. Lewis acid catalyzed photoaddition of benzyltrimethylsilane and tetramethyltin via photoinduced electron transfer. *J. Am. Chem. Soc. 123*, 7756−7766.
(39) Mann, C. K., and Barnes, K. K. (1970) *Electrochemical Reactions in Non Aqueous Systems*, Mercel Dekker, New York.
(40) Sheldon, R. A. (1993) In *The Activation of Dioxygen and Homogeneous Catalytic Oxidation* (Barton, D. H. R., Martell, A. E., and Sawyer, D. T., Eds.) pp 9−30, Plenum Press, New York and London.
(41) Parshall, G. W., and Ittel, S. D. (1992) *Homogeneous Catalysis*, 2nd ed., Chapter 10, Wiley, New York.
(42) Sheldon, R., and Kochi, J. K. (1976) Metal catalyzed oxidations of organic compounds in the liquid phase: a mechanistic approach. *Adv. Catal. 25*, 272−413.
(43) Shilov, A. E. (1984) *Activation of Saturated Hydrocarbons by Transition Metal Complexes*, Chapter 4, D. Reidel Publishing Co., Dordrecht, The Netherlands.
(44) Böttcher, A., Birnbaum, F. R., Day, M. W., Gray, H. B., Grinstaff, M. W., and Labinger, J. A. (1997) How do electronegative substituents make metal complexes better catalysts for the oxidation of hydrocarbons by dioxygen? *J. Mol. Catal. A 117*, 229−242.
(45) Kochi, J. K. (1957) *Free Radicals in Solution*, John Wiley & Sons, New York.
(46) Kochi, J. K., Krusic, P. J., and Eaton, D. R. (1969) Homoallylic rearrangement and electron spin resonance of cyclopropylcarbinyl radicals. *J. Am. Chem. Soc. 91*, 1877−1879.
(47) Kochi, J. K., and Krusic, P. J. (1968) Electron spin resonance of aliphatic hydrocarbon radicals in solution. *J. Am. Chem. Soc. 90*, 7155−7157.
(48) Kochi, J. K., and Krusic, P. J. (1969) Electron spin resonance of organosilyl radicals in solution. *J. Am. Chem. Soc. 91*, 3938−3940.
(49) Kochi, J. K., and Krusic, P. J. (1969) Electron spin resonance studies of homolytic substitution reactions. Oraganoboron, aluminum, and gallium compounds. *J. Am. Chem. Soc. 91*, 3942−3944.
(50) Kochi, J. K., and Krusic, P. J. (1969) Displacement of alkyl groups from organophosphorus compounds studied by electron spin resonance. *J. Am. Chem. Soc. 91*, 3944−3946.
(51) Howard, J. A., and Furimsky, E. (1974) Electron spin resonance study on the *tert* butylsulfinyl radical. *Can. J. Chem. 52*, 555−556.
(52) Fukuzumi, S., and Ono, Y. (1977) Decay kinetics of cumylperoxyl radical produced by the decomposition of cumene hydroperoxide. *J. Chem. Soc., Perkin Trans. 2*, 622−625.
(53) Fukuzumi, S., and Ono, Y. (1977) Electron spin resonance and kinetic studies on the liquid phase autoxidation of cumene with lead dioxide. *J. Chem. Soc., Perkin Trans. 2*, 784−788.
(54) Watanabe, T., Yuki, S., Egawa, M., and Nishi, H. (1994) Protective effects of MCI 186 on cerebral ischemia: possible involvement of free radical scavenging and antioxidant actions. *J. Pharmacol. Exp. Ther. 268*, 1597−1604.
(55) Yamamoto, T., Yuki, S., Watanabe, T., Mitsuya, M., and Saito, K. (1997) Delayed neuron death prevented by inhibition of increased hydroxyl radical formation in a transient cerebral ischemia. *Brain Res. 762*, 240−242.
(56) Okatani, Y., Wakatsuki, A., Enzan, H., and Miyahara, Y. (2003) Edaravone protects against ischemia/reperfusion induced oxidative damage to mitochondria in rat liver. *Eur. J. Pharmacol. 465*, 163−170.
(57) Thomas, J. P., Totsch, K. D., Cleary, J. F., Bailey, H. H., Arzoomanian, R., Alberti, D., Simon, K., Feierabend, C., Binger, K., Marnocha, R., Dresen, A., and Wilding, G. (2002) Phase I clinical and pharmacokinetic trial of the cyclin dependent kinase inhibitor flavopiridol. *Cancer Chemother. Pharmacol. 50*, 465−472.
(58) Kouroukis, C. T., Belch, A., Crump, M., Eisenhauer, E., Gascoyne, R. D., Meyer, R., Lohmann, R., Lopez, P., Powers, J., Turner, R., and Connors, J. M. (2003) Flavopiridol in untreated of relapsed mantle cell lymphoma: results of a phase II study of the National Cancer Institute of Canada Clinical Trials Group. *J. Clin. Oncol. 21*, 1740−1745.
(59) Senderowicz, A. M. (2002) Cyclin dependent kinases as new targets for the prevention and treatment of cancer. *Hematol. Oncol. Clin. North Am. 16*, 1229−1253.
(60) Ngnokam, D., Massiot, G., Nuzillard, J. M., and Tsamo, E. (1994) (+) 7′,7′ Dimethyl 5 hydroxy 2R,3S trans pubeschin from *Entada drophragma cylindricum*. *Phytochemistry 37*, 529−531.
(61) Davis, K. J. A. (1996) Oxidative stress: The paradox of aerobic life. *Biochem. Soc. Symp. 61*, 1−31.
(62) Nakanishi, I., Fukuhara, K., Shimada, T., Ohkubo, K., Iizuka, Y., Inami, K., Mochizuki, M., Urano, S., Itoh, S., Miyata, N., and Fukuzumi, S. (2002) Effects of magnesium ion on kinetic stability and spin distribution of phenoxyl radical derived from a vitamin E analogues: mechanistic insight into antioxidative hydrogen transfer reaction of vitamin E. *J. Chem. Soc., Perkin Trans. 2*, 1520−1524.
(63) Fukuzumi, S., Shimoosako, K., Suenobu, T., and Watanabe, Y. (2003) Mechanism of hydrogen , oxygen , and electron transfer reactions of cumylperoxyl radical. *J. Am. Chem. Soc. 125*, 9074−9082.
(64) Itoh, S., Kumei, H., Nagatomo, S., Kitagawa, T., and Fukuzumi, S. (2001) Effects of metal ions on physicochemical properties and redox reactivity of phenolates and phenoxyl radicals: mechanistic insight into hydrogen atom abstraction by phenoxyl radical metal complexes. *J. Am. Chem. Soc. 123*, 2165−2175.
(65) Itoh, S., Maruta, J., and Fukuzumi, S. (1996) Addition cyclization reaction of nitroalkane anions with *o* quinone derivatives via electron transfer in the charge transfer complexes. *J. Chem. Soc., Perkin Trans. 2*, 1429−1433.
(66) Boozer, C. E., and Hammond, G. S. (1954) Molecular complex formation in free radical reactions. *J. Am. Chem. Soc. 76*, 3861−3862.
(67) Boozer, C. E., Hammond, G. S., Hamilton, C. E., and Sen, J. N. (1955) Air oxidation of hydrocarbons. II. The stoichiometry and fate of inhibitors in benzene and chlorobenzene. *J. Am. Chem. Soc. 77*, 3233−3237.

TX034134C

A Planar Catechin Analogue as a Promising Antioxidant with Reduced Prooxidant Activity

Kiyoshi Fukuhara,*,[†] Ikuo Nakanishi,*,[†] Tomokazu Shimada,[†,§] Kei Ohkubo,[∥] Kentaro Miyazaki,[†,§] Wataru Hakamata,[†] Shiro Urano,[§] Toshihiko Ozawa,[†] Haruhiro Okuda,[†] Naoki Miyata,[⊥] Nobuo Ikota,*,[†] and Shunichi Fukuzumi*,[∥]

Division of Organic Chemistry, National Institute of Health Sciences, Setagaya-ku, Tokyo 158-8501, Japan, Redox Regulation Research Group, Research Center for Radiation Safety, National Institute of Radiological Sciences, Inage-ku, Chiba 263-8555, Japan, Department of Applied Chemistry, Shibaura Institute of Technology, Minato-ku, Tokyo 108-8548, Japan, Department of Material and Life Science, Graduate School of Engineering, Osaka University, CREST, Japan Science and Technology Corporation, Suita, Osaka 565-0871, Japan, and Department of Organic and Medicinal Chemistry, Graduate School of Pharmaceutical Sciences, Nagoya City University, Mizuho-ku, Nagoya 467-8603, Japan

Received July 18, 2002

A planar catechin analogue (**1H$_2$**), in which catechol and chroman moieties in (+)-catechin are constrained to be coplanar, is an efficient radical scavenger compared to the native catechin, and are nearly as effective as quercetin, a strong radical scavenger. The dianion (**1^{2-}**) of **1H$_2$** produced by the reaction of **1H$_2$** with 2 equiv of tetramethylammonium methoxide reduced molecular oxygen (O_2) to generate superoxide anion ($O_2^{\bullet-}$). The resulting radical anion (**1$^{\bullet-}$**) from **1H$_2$** underwent intramolecular proton transfer to give an *o*-semiquinone radical anion form of **1$^{\bullet-}$**, which shows a characteristic ESR spectrum with *g* value of 2.0048. Although the same mechanism has also been shown for (+)-catechin, the rate constant of electron transfer (k_{et}) from **1^{2-}** to O_2 is about a half of that reported for (+)-catechin, indicating that the electron transfer from **1^{2-}** to O_2 is slower than that from (+)-catechin dianion to O_2. Together with efficient protection against DNA strand breakage induced by the Fenton reaction, the small k_{et} value for **1H$_2$** implies that, in physiologically relevant systems, there is less of a possibility of generating oxygen radicals responsible for prooxidant activity with **1H$_2$** than that with (+)-catechin. The strong radical scavenging ability and less efficient generation of $O_2^{\bullet-}$ suggest that the planar catechin analogue may be useful for the prevention and/or treatment of free radical associated diseases.

Introduction

Flavonoids are plant phenolic compounds that are widely distributed in foods and beverages (*1*). They have been extensively studied with regard to their antioxidative and cytoprotective properties in various biological models (*2*–*5*). They can protect against oxidative stress by scavenging reactive oxygen intermediates (*6*–*8*) and also by chelating iron (*9*). Since oxidative damage to biomolecules, such as DNA and carbohydrate, proteins, or polyunsaturated fatty acids is thought to play a significant role in mutagenesis, cancer, aging, and other human pathologies, considerable attention has been focused on the development of antioxidants to prevent or to treat diseases associated with oxidative stress (*3*, *10*). However, there is also some evidence that flavonoids themselves are mutagenic (*11*–*14*) and carcinogenic (*15*, *16*) in both bacterial and mammalian experimental systems. The process that damages DNA, and is thus responsible for DNA alterations and genotoxicity, could be accelerated by the effects of metal ions, as naturally occurring metal constituents of the nucleus. Indeed, while quercetin is known to be a powerful antioxidant that scavenges free radicals associated with lipid peroxidation, the dietary administration of excessive quercetin has been reported to induce renal tubule adenomas and adenocarcinomas in male rats (*15*), as well as intestinal and bladder cancer in rats (*16*). There is also considerable evidence that quercetin induces extensive DNA damage and forms 8-oxodG by reacting with Cu(II) (*17*). Therefore, to develop an antioxidant for clinical use, a compound having a strong antioxidative activity but with a weak prooxidant effect has been desired.

(+)-Catechin, one of typical flavonoids, widely distributed in the plant kingdom is known to be a powerful antioxidant (*5*, *18*) and its biological and pharmacological properties have recently received increasing attention (*19*–*21*). However, there is little evidence that the antioxidant activity of (+)-catechin is sufficient for the treatment of diseases associated with oxidative stress. In the presence of Cu(II) and molecular oxygen (O_2), (+)-catechin has been shown to promote extensive DNA cleavage and fatty acid peroxidation (*22*). In support of its prooxidant activity, it has been reported that the dianion of (+)-catechin produced in the reaction between (+)-catechin and 2 equiv of tetramethylammonium meth-

* To whom correspondence should be addressed. Phone: 81-3-3700-1141. Fax: 81-3-3707-6950. E-mail: fukuhara@nihs.go.jp.
† National Institute of Health Sciences.
‡ National Institute of Radiological Sciences.
§ Shibaura Institute of Technology.
∥ Osaka University, CREST, Japan Science and Technology Corporation.
⊥ Nagoya City University.

10.1021/tx025581f CCC: $25.00
Published on Web 12/18/2002

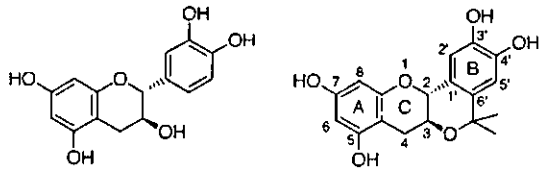

Figure 1. Chemical structures of (+) catechin and planar catechin ($\mathbf{1H_2}$).

oxide reduces O_2 to generate superoxide anion ($O_2^{\bullet}$) (*23*). The prooxidative activity responsible for the generation of radicals of several types may reduce the net effect of the antioxidative activity in free radical associated events. Recently, we have synthesized a novel planar catechin analogue ($\mathbf{1H_2}$), in which the geometry of (+) catechin is constrained to be planar (Figure 1) (*24*). The $\mathbf{1H_2}$ shows strong radical scavenging ability compared to (+) catechin and efficiently protects against DNA strand breakage induced by the Fenton reaction (*24*). In this study, we examined the generation of $O_2^{\bullet}$ in the reaction between the dianion ($\mathbf{1^{2}}$) of $\mathbf{1H_2}$ and O_2 under basic conditions. The extent of $O_2^{\bullet}$ generation and valuable mechanistic details were discussed by detailed spectroscopic and kinetic analyses. The structure of the radical anion ($\mathbf{1^{\bullet}}$) formed via electron transfer from $\mathbf{1^{2}}$ to O_2 was also well characterized by ESR analyses and theoretical calculations. Its capacity for $O_2^{\bullet}$ generation, which is estimated to be about a half as that of (+) catechin, as well as its antioxidant properties, may make it useful for the treatment of free radical associated diseases.

Materials and Methods

Materials. A planar catechin analogue ($\mathbf{1H_2}$) was synthesized via an oxa Pictet–Spengler reaction using (+) catechin and acetone with $BF_3{\bullet}Et_2O$ as a Lewis acid (25). (+) Catechin was purchased from Sigma-Aldrich Chemical Co.(St. Louis, MO), and purified using silica gel column chromatography, eluting with toluene/acetone/methanol (7:3:1 v/v). The purity of each compound was confirmed by NMR analysis to be greater than 98% as determined by the integration of peak signals. Tetrabutylammonium hydroxide (Bu_4NOH) (1.0 M in methanol) was obtained commercially from Aldrich and used as received. Acetonitrile (MeCN; spectral grade) used as a solvent was purchased from Nacalai Tesque, Inc., Japan.

Spectral and Kinetic Measurements. Since the dianion of the planar catechin analogue ($\mathbf{1^{2}}$) is readily oxidized by dioxygen, reactions were carried out under strictly deaerated conditions. A continuous flow of Ar gas was bubbled through a MeCN solution containing $\mathbf{1H_2}$ (1.5×10^{-4} M) in a square quartz cuvette (10 mm i.d.) for 10 min. The neck of the cuvette was then sealed with a rubber septum and Parafilm under Ar to ensure that air would not leak into the cuvette. A microsyringe was used to inject 2 equiv of Bu_4NOMe (3.0×10^{-4} M), which was also deaerated, into the cuvette to produce $\mathbf{1^{2}}$. UV–vis spectral changes associated with this reaction were monitored using a Hewlett–Packard 8453 photodiode array spectrophotometer. The reaction of $\mathbf{1^{2}}$ with O_2 was carried out by adding a stock solution of $\mathbf{1^{2}}$ to an MeCN solution of O_2 in the cuvette. The concentration of O_2 in the solution was adjusted by purging with Ar, air, or O_2 for 10 min prior to the measurements ([O_2] 0, 2.7×10^{-3}, or 1.3×10^{-2} M, respectively). The rates of electron transfer from $\mathbf{1^{2}}$ to O_2 were determined by monitoring the absorbance change at 485 nm ($\varepsilon = 1.77 \times 10^{3}$ M^{-1} cm^{-1}) due to $\mathbf{1^{\bullet}}$. Pseudo first order or second order rate constants were determined by least squares curve fitting using an Apple Macintosh personal computer. The first order plots of ln($A_\infty - A$) vs time (where A_∞ and A denote the final absorbance and the absorbance at a given reaction time, respectively) were linear for three or more half lives, with a correlation coefficient of $\rho > 0.999$.

ESR Measurements. To an oxygen saturated MeCN solution was added the stock MeCN solution of $\mathbf{1^{2}}$ (1.5×10^{-4} M) in a quartz ESR tube (4.5 mm i.d.) and the solution was immediately frozen by liquid nitrogen. The ESR spectra of $O_2^{\bullet}$ were taken in frozen MeCN solution at 77 K with a JEOL X-band spectrometer (JES-FA100) under nonsaturating microwave power conditions. The g values were calibrated precisely with a Mn^{2+} marker which was used as a reference. The ESR spectrum of $\mathbf{1^{\bullet}}$, which was produced by the reaction between $\mathbf{1^{2}}$ (3.2×10^{-3} M) and O_2 (1.3×10^{-2} M) in MeCN in a LABOTEC LLC 04B ESR sample tube was measured at 298 K. Computer simulation of the ESR spectrum was carried out using Calleo ESR Version 1.2 (Calleo Scientific Publisher) on an Apple Macintosh personal computer.

Theoretical Calculations. The semiempirical calculations by the PM3 method were performed on a COMPAQ DS20E computer. Final geometries and energetics were obtained by optimizing the total molecular energy with respect to all structural variables. The geometries of the radicals were optimized using the unrestricted Hartree–Fock (UHF) formalism formalism as implemented in the Gaussian 98 program (*26*).

Density functional calculations were performed on a COMPAQ DS20E computer using the Amsterdam Density Functional (ADF) program version 1999.02 developed by Baerends et al. (*27, 28*). The electronic configurations of the molecular systems were described by an uncontracted triple ζ Slater type orbital basis set (ADF basis set IV), with a single polarization function used for each atom. Core orbitals were frozen through 1s (C, O). The calculations were performed using the local exchange correlation potential of Vosko et al. (*29*) and the nonlocal gradient corrections of Becke (*30*) and Perdew (*31, 32*) during the geometry optimizations. First order scalar relativistic corrections were added to the total energy. Final geometries and energetics were optimized using the algorithm of Versluis and Ziegler (*33*) provided in the ADF package and were considered to be converged when the changes in bond lengths between subsequent iterations fell below 0.01 Å.

Results

Formation of a Dianion of $\mathbf{1H_2}$ in the Reaction of $\mathbf{1H_2}$ with MeO$^-$. When one equivalent of methoxide anion (MeO$^-$) produced in the reaction between tetra-*n*-butylammonium hydroxide and methanol was added to a deaerated acetonitrile (MeCN) solution of $\mathbf{1H_2}$, the absorption band at 281 nm due to $\mathbf{1H_2}$ shifted to 299 nm (Figure 2). A similar spectral change was observed upon the addition of 1 equiv of MeO$^-$ to (+) catechin to produce the corresponding phenolate anion in deaerated MeCN (*23*). Since the first deprotonation of (+) catechin is known to occur at the OH group at the C 3′ position on the B ring (*34*), the reaction of $\mathbf{1H_2}$ with MeO$^-$ can be described as shown in Scheme 1, where the anion of $\mathbf{1H_2}$ ($\mathbf{1H^-}$) is formed.

Since the pK_a value of the OH group at C 7 position is very close to that of C 3′ OH group [9.26 and 8.97, respectively, in the case of (+) catechin (*34*)], $\mathbf{1H_2}$ may be in equilibrium with an another anion species, where the OH group at C 7 position is deprotonated as shown in Scheme 1. This is why no isosbestic point is observed in Figure 1.

The addition of 2 equiv of MeO$^-$ to $\mathbf{1H_2}$ resulted in an increase in the absorption band at 299 nm, accompanied by an increase in the absorbance at around 340 nm as a shoulder (Figure 2). The absorption band at around 340 nm is typical for the phenolate anion of resorcinol (*34*),

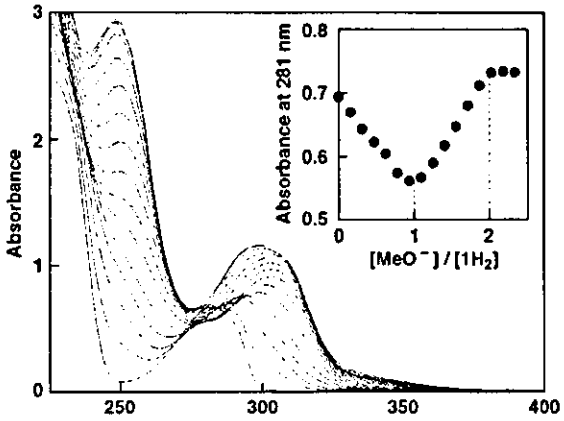

Figure 2. Spectral change upon the addition of MeO⁻ (3.0 × 10⁻⁴ M) to a deaerated MeCN solution of $\mathbf{1H_2}$ (1.5 × 10⁻⁴ M) at 298 K. (Inset) Plot of the absorbance change at 281 nm against [MeO⁻]/[$\mathbf{1H_2}$].

Scheme 1

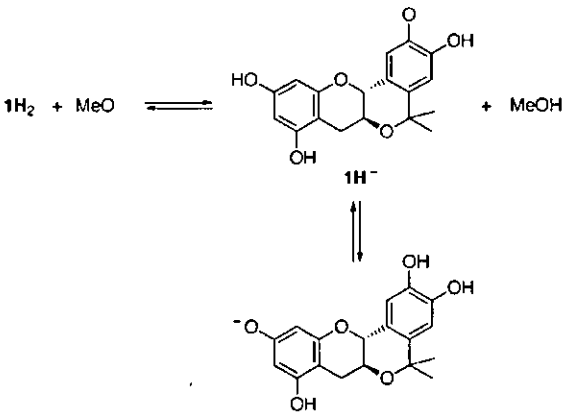

Scheme 2

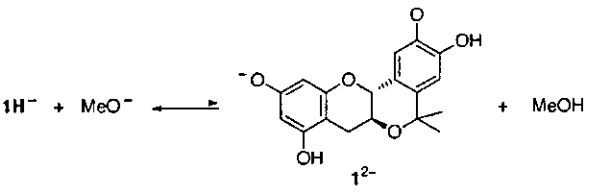

indicating that the second deprotonation of $\mathbf{1H_2}$ takes place at the OH group at C 7 on the A ring to produce the dianion $\mathbf{1^{2-}}$, as in the case of (+) catechin (Scheme 2) (*23*).

Thus, $\mathbf{1H_2}$ reacts with 2 equiv of MeO⁻ to form the corresponding dianion $\mathbf{1^{2-}}$. The stoichiometry of the reaction was confirmed by the plot of absorbance at 281 nm vs [MeO⁻]/[$\mathbf{1H_2}$], where $\mathbf{1H_2}$ reacts with 2 equiv of MeO⁻ in a stepwise manner (inset in Figure 2). The resulting $\mathbf{1^{2-}}$ is stable under anaerobic conditions.

Superoxide Anion Formation by the Reaction of $\mathbf{1^{2-}}$ with $\mathbf{O_2}$. Introduction of molecular oxygen (O_2) to the MeCN solution of $\mathbf{1^{2-}}$ resulted in an increase in the absorption bands at 485 and 635 nm, as shown in Figure 3.

This spectral change suggests that $\mathbf{1^{2-}}$ is oxidized by O_2 to produce the radical anion $\mathbf{1^{\bullet-}}$ and superoxide anion ($O_2^{\bullet-}$) (*23*). In fact, an ESR spectrum with a g value of

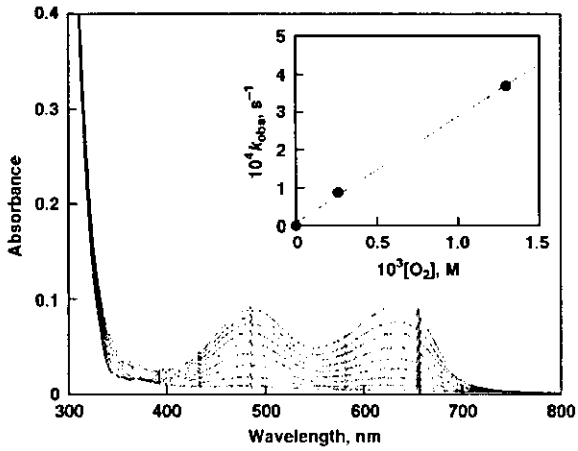

Figure 3. Spectral change observed in the reaction of $\mathbf{1^{2-}}$ (1.5 × 10⁻⁴ M) with O_2 (1.3 × 10⁻² M) in MeCN at 298 K. (Inset) Plot of k_{obs} vs [O_2].

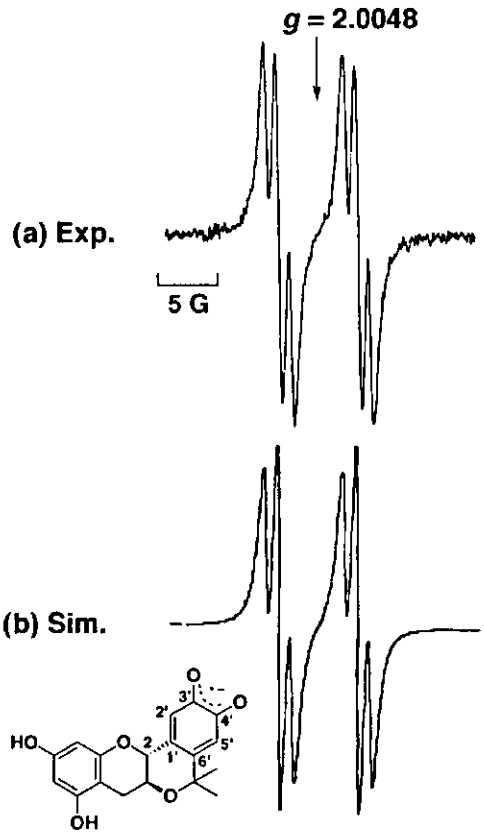

Figure 4. (a) ESR spectrum of $\mathbf{1^{\bullet-}}$ generated in the reaction of $\mathbf{1^{2-}}$ (3.2 × 10⁻³ M) with O_2 (1.3 × 10⁻² M) in MeCN at 298 K. (b) Computer simulated spectrum with g 2.0048, a(H⁴) 6.60 G, a(H²′) 1.10 G, a(H⁶′) 1.10 G, ΔH_{msl} 0.6 G. The calculated hfs values of $\mathbf{1^{\bullet-}}$ using the ADF method are a(H⁴) 6.6 G, a(H²′) 3.9 G, a(H⁶′) 3.5 G.

2.0048 was observed in the reaction of $\mathbf{1^{2-}}$ with O_2 in MeCN at 298 K, as shown in Figure 4a.

The observed hyperfine structure in Figure 4a is well reproduced by the computer simulation (Figure 4b), with the hyperfine splitting (hfs) values of three nonequivalent protons (6.64, 1.10, and 1.10 G). In the case of (+) catechin, *o* semiquinone radical anion of (+) catechin is

Table 1. Heats of Formation (ΔH_f) of $1^{\bullet}$ Calculated by the PM3 Method

$1^{\bullet-}$	ΔH_f, kcal mol^{-1}
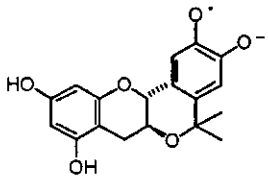	−230.5
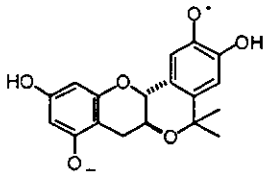	−220.7
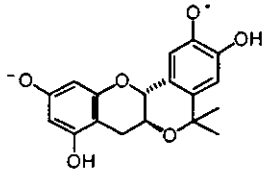	−221.6
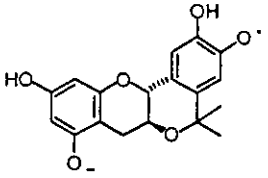	−215.4
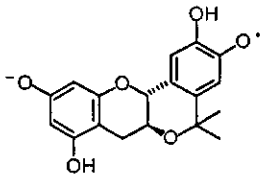	−216.3
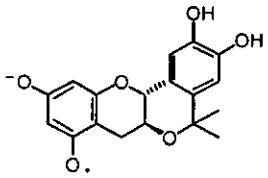	−219.9

generated via an electron transfer from the dianion of (+) catechin to O_2 followed by intramolecular proton transfer in the radical anion of (+) catechin (*23*). There are six possible forms of $1^{\bullet}$. MO calculations using the PM3 method (*35*) were performed for the six possible $1^{\bullet}$ and the calculated heats of formation (ΔH_f) are listed in Table 1.

As in the case of (+) catechin, the *o* semiquinone radical anion form of $1^{\bullet}$ is most stable based on its most negative ΔH_f value. On the basis of the calculated spin density of $1^{\bullet}$ using the Amsterdam Density Functional (ADF) method (see Experimental Section), we assigned the hfs values as shown in Figure 4. As in the case of (+) catechin (*23*), these results indicate that intramolecular proton transfer takes place after electron transfer oxidation of O_2 to produce the *o* semiquinone radical anion form of $1^{\bullet}$ (Scheme 3).

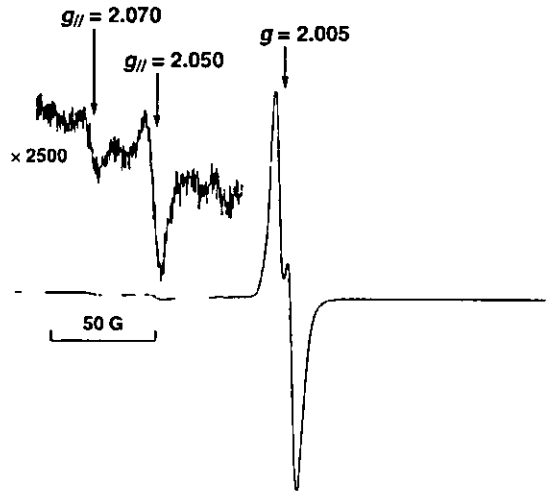

Figure 5. ESR spectrum of $O_2^{\bullet}$ generated in the reaction of $\mathbf{1H_2}$ (3.4×10^{-3} M) with O_2 (1.3×10^{-2} M) in MeCN at 298 K and measured at 77 K.

It has been reported that hfs values for benzylic methylene protons of phenoxyl radicals can be estimated by the angle dependent McConnel type relationship, as given by eq 1

$$a_{C\text{-}H} = \rho_{C1'} B \cos^2\theta \qquad (1)$$

where $a_{C\text{-}H}$ is the hfs value of methylene proton, $\rho_{C1'}$ is the spin density at the C1′ position, B is a constant equal to 162 Hz, and θ ($0 \le \theta \le 90°$) is the dihedral angle defined in Figure 8 of Babcock's paper (*36*).

According to eq 1, a greater $a_{C\text{-}H}$ value is associated with a smaller θ. Thus, the relatively large hfs value due to the benzylic proton (6.60 G) of $1^{\bullet}$ compared to that of the radical anion of (+) catechin (1.50 G) indicates that $\mathbf{1H_2}$ is planar.

The formation of $O_2^{\bullet}$ in the electron transfer oxidation of $\mathbf{1^2}$ by O_2 was confirmed by a low temperature ESR. A characteristic ESR signal having $g_{//}$ value of 2.070 due to $O_2^{\bullet}$ together with an ESR signal with a $g_{//}$ value of 2.050 for protonated $O_2^{\bullet}$ ($HO_2^{\bullet}$) were observed for an O_2 saturated MeCN solution of $\mathbf{1H_2}$ and 2 equiv of MeO$^-$ at 77 K, as shown in Figure 5 (*36*).

The increase in absorbance at 485 nm due to $1^{\bullet}$ obeyed pseudo first order kinetics under conditions where the O_2 concentration was maintained at more than a 10 fold excess relative to the $\mathbf{1^2}$ concentration. The pseudo first order rate constant (k_{obs}) increases linearly with an increase in the O_2 concentration, as shown in the inset in Figure 3. The slope of the linear plot of k_{obs} vs $[O_2]$ gave the second order rate constant of the electron transfer (k_{et}) from $\mathbf{1^2}$ to O_2: 2.8×10^{2} M^{-1} s^{-1}. This k_{et} value is about half of that determined for (+) catechin (5.8×10^{2} M^{-1} s^{-1}).

Scheme 3

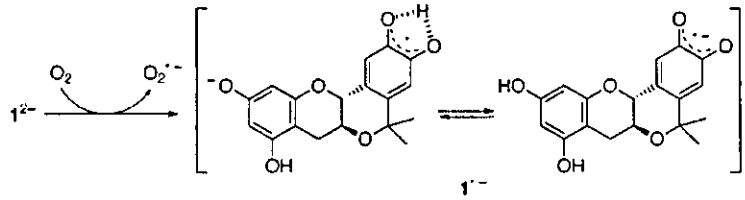

Although, the direct determination of the oxidation potential (E^0_{ox}) of $\mathbf{1}^{2-}$ by cyclic voltammetry was precluded due to the strong adsorption of electrolyzed products of $\mathbf{1}^{2-}$, the relatively small k_{et} value indicates that electron transfer from $\mathbf{1}^{2-}$ to O_2 (E^0_{red} vs SCE = −0.87 V) is endergonic ($\Delta G^0_{et} = e(E^0_{ox} - E^0_{red}) > 0$, where e is the elementary charge). Thus, the follow up reaction, which involves an intramolecular proton transfer from the OH group in the B ring to the phenolate anion of the A ring, is exothermic and makes the electron transfer from $\mathbf{1}^{2-}$ to O_2 possible to produce $O_2^{\bullet-}$.

Discussion

The antioxidative and metal chelating effects of flavonoids undoubtedly contribute to their antimutagenic and chemopreventive activities. However, the fact that flavonoids themselves have been shown to have antibacterial and bactericidal activities, as well as being mutagenic and procarcinogenic, should be considered when contemplating their clinical use. Their harmful effects are thought to be due to their prooxidant activities (*38*−*40*). Therefore, when a new type of antioxidant is developed, it is also very important to consider how its prooxidant properties can be reduced. The objective of the current study was to examine the relative abilities of $\mathbf{1H_2}$ and native catechin to produce superoxide anion in response to their prooxidant activities.

In the presence of Cu(II), (+) catechin has been shown to damage cytoplasmic membrane, which is related to its bactericidal activity. The (+) catechin/Cu(II) system induces oxidative DNA damage and fatty acid peroxidation and also shows prooxidant activity resulting from reactive oxygen species via electron transfer from (+) catechin to molecular oxygen, which is mediated by Cu(II). The participation of Cu(II) may be essential for the prooxidant activity of (+) catechin and plays a part in mediating the reductive activation of molecular oxygen by (+) catechin. However, if a dianion of (+) catechin is formed under basic conditions, molecular oxygen is readily reduced to form $O_2^{\bullet-}$. Considering the pK_a of (+) catechin, the dianion represents only about 1/1000 of (+) catechin at pH 7.0. However, the prooxidant effect involving the generation of reactive oxygen cannot be neglected even under physiological conditions. In fact, at pH 7.4, (+) catechin itself can induce DNA strand scission, which is attributed to the generation of oxygen radicals(data not shown).

The radical scavenging ability of $\mathbf{1H_2}$ is excellent compared to that of (+) catechin and is almost comparable to that of quercetin (*24*). A great advantage of $\mathbf{1H_2}$, compared with catechin or quercetin, is its lack of prooxidant activity, which precludes the clinical application of quercetin. Indeed, the present data demonstrated that the dianion of $\mathbf{1H_2}$ is produced in the reaction between $\mathbf{1H_2}$ and 2 equiv of tetramethylammonium methoxide, and $O_2^{\bullet-}$ is formed via one electron oxidation of the dianion to generate $\mathbf{1}^{\bullet-}$, followed by intramolecular proton transfer to the *o* semiquinone radical anion of $\mathbf{1}^{\bullet-}$. The same mechanism has been seen with (+) catechin. That is, the rate of electron transfer from each dianion of $\mathbf{1H_2}$ and catechin to molecular oxygen shows first order dependence, indicating that one molecule of dianions reacts with one molecule of O_2, respectively. However, the k_{et} value for $\mathbf{1H_2}$ is about half that for (+) catechin, indicating that electron transfer from $\mathbf{1}^{2-}$ to O_2 proceeds slowly compared to that with (+) catechin. The antioxidative abilities of polyphenol derivatives concomitant with electron transfer depend on their electron donating properties. The electron donating properties of polyphenol are also responsible for the facile production of superoxide by reduction of molecular oxygen under basic condition. Indeed, quercetin ($E_{1/2} = 0.06$ V vs SCE), which is a stronger reductant than catechin ($E_{1/2} = 0.15$ V vs SCE) (*41*), not only reacts faster than catechin with $C^{\bullet}$ but also easily reduces oxygen to generate large amount of superoxide anion under basic condition (data not shown). The most striking outcome of the present experiments is that k_{et} value of the $\mathbf{1}^{2-}$−O_2 system is much smaller than that of dianion of catechin−O_2 system though the radical scavenging ability of $\mathbf{1H_2}$ is increased. While it provides efficient protection against DNA strand breakage induced by the Fenton reaction, the low k_{et} value for $\mathbf{1H_2}$ implies that, in physiologically relevant systems, the ability of $\mathbf{1H_2}$ to generate oxygen radicals responsible for its prooxidant activity might not be as high as that of (+) catechin. Among natural antioxidants, α tocopherol and ascorbic acid are typical compounds which are recently useful for the treatment or prevention of diseases associated with oxidative stress. However, administrating a large amount of such antioxidants may be unfavorable because of their prooxidant properties (*42*, *43*), such as (+) catechin or quercetin. Therefore, the use of $\mathbf{1H_2}$, rather than natural antioxidant such as (+) catechin, quercetin, tocopherol, ascorbic acid, etc., might be favorable for the treatment of diseases associated with oxidative stress because of the suppression of oxidant injury as side effect arising form antioxidant itself.

In conclusion, $\mathbf{1H_2}$, in which the catechol and chroman in (+) catechin are constrained to be coplanar, was found to be much less effective for $O_2^{\bullet-}$ generation under basic conditions and was a strong radical scavenger. The unique characteristics responsible for its antioxidant ability suggest that this planar catechin analogue may be useful for the prevention and/or treatment of free radical associated diseases.

Acknowledgment. This work was supported in part by a grant from the Health Sciences Foundation from the Ministry of Health, Labor and Welfare of Japan and by a Grants in Aid for Scientific Research from the Ministry of Education, Science, Sports and Culture of Japan.

References

(1) Kühnau, J. (1976) The flavonoids. A class of semi essential food components: their role in human nutrition. *Word Rev. Nutr. Diet* **24**, 117−191.

(2) Havsteen, B. (1983) Flavonoids, a class of natural products of high pharmacological potency. *Biochem. Pharmacol.* **32**, 1141−1148.

(3) Terao, J., Piskula, M., and Yao, Q. (1994) Protective effect of epicatechin, epicatechin gallate and quercetin on lipide peroxidation in phospholipid bilayers. *Arch. Biochem. Biophys.* **308**, 278−284.

(4) Salah, N., Miller, N. J., Paganga, G., Tijburg, L., and Bolwell, G. P., Rice Evans, C. A. (1995) Polyphenolic flavonoids as scavengers of aqueous phase radicals and as chain breaking antioxidants. *Arch. Biochem. Biophys.* **322**, 339−346.

(5) Rice Evans C. A., Miller, N. J., and Paganga, G. (1996) Structure antioxidant activity relationships of flavonoids and phenolic acids. *Free Radical Biol. Med.* **20**, 933−956.

(6) Jovanovic, S. V., Streenken, S., Tosic, M., Marjanovic, B., and Simic, M. G. (1994) Flavonoids as antioxidants. *J. Am. Chem. Soc.* **116**, 4846−4851.

(7) Hanasaki, Y., Ogawa, S., and Fukui, S. (1994) The correlation between active oxygen scavenging and antioxidative effects of flavonoids. *Free Radical Biol. Med.* **16**, 845−850.

(8) Hu, J. P., Calomme, M., Lasure, A., De Bruyne, T., Pieters, L., Vlietinck, A., and Vanden Berghe, D. A. (1995) Structure−activity relationships of flavonoids with superoxide scavenging ability. *Biol. Trace. Elem. Res* **47**, 327−331.

(9) Morel, I., Lescoat, G., Cogrel, O., Sergent, O., Pasdeloup, N., Brissot, P., Cillard, P., and Cillard, J. (1993) Antioxidant and iron chelating activities of the flavonoids catechin, quercetin and diosmetin on iron loaded rat hepatocyte cultures. *Biochem. Pharmacol.* **45**, 13−19.

(10) Elangovan, V., Sekar, N., and Govindasamy, S. (1994) Chemopreventive potential of dietary bioflavonoids against 20 methyl cholanthrene induced tumorigenesis. *Cancer Lett.* **87**, 107−113.

(11) Ochiai, M., Nagao, M., Wakabayashi, K., and Sugimura, T. (1984) Superoxide dismutase acts an enhancing factor for quercetin mutagenesis in rat liver cytosol by preventing its decomposition. *Mutat. Res.* **129**, 19−24.

(12) Rueff, J., Laires, A., Borba, H., Chaveca, T., Gomes, M. L., and Halpern, M. (1986) Genetic toxicology of flavonoids: the role of metabolic conditions in the induction of reverse mutation, SOS functions and sister chromatid exchanges. *Mutagenesis* **1**, 179−183.

(13) Popp, R., and Schimmer, O. (1991) Induction of sister chromatid exchanges (SCE), polyploidy, and micronuclei by plant flavonoids in human lymphocyte cultures. A comparative study of 19 flavonoids. *Mutat. Res.* **246**, 205−213.

(14) Salim, S. C., and Washington M. C. (1991) Effects of antioxidants on quercetin induced nuclear DNA damage and lipid peroxidation. *Cancer Lett.* **60**, 259−264.

(15) Pamukcu, A. M., Yalciner, S., Hatcher, J. F., and Bryan, G. T. (1980) Quercetin, a rat intestinal and bladder carcinogen present in bracken fern (*Pteridium aquilinum*). *Cancer Res.* **40**, 3468−3472.

(16) Toxicology and carcinogenesis studies of quercetin in F344 rats (1992) National Toxicology Program (NTP) Technical Report, NTP TR 409, NIH publication no. 93 147478.

(17) Yamashita, N., Tanemura, H., and Kawanishi, S. (1999) Mechanism of oxidative DNA damage induced by quercetin in the presence of Cu(II). *Mutat. Res.* **425**, 107−115.

(18) Huang, S. W., and Frankel, E. N. (1997) Antioxidant activity of tea catechins in different lipid system. *J. Agric. Food Chem.* **45**, 3033−3038.

(19) Ikigai, H., Nakae, T., Hara, Y., and Shimamura, T. (1993) Bactericidal catechins damage the lipid bilayer. *Biochim. Biophys. Acta* **1147**, 132−136.

(20) Anderson R. F., Anarasinghe, C., Fisher, L. J., Mak, W. B., and Packer, J. E. (2000) Reduction in free radical induced DNA strand breaks and base damage last chemical repair by flavonoids. *Free Radical Res.* **33**, 91−103.

(21) Ratna, W. N., and Simonelli, J. A. (2002) The action of dietary phtochemicals quercetin, catechin, resveratrol and naringenin on etrogen mediated gene expression. *Life Sci.* **70**, 1577−1589.

(22) Hayakawa, F., Kimura, T., Maeda, T., Fujita, M., Sohmiya, H., and Ando, T. (1997) DNA cleavage reaction and linoleic acid peroxidation induced by tea catechins in the presence of cupric ion. *Biochim. Biophys. Acta* **1336**, 123−131.

(23) Nakanishi, I., Fukuhara, K., Ohkubo, K., Shimada, T., Kansui, H., Kurihara, M., Urano, S., Fukuzumi, S., and Miyata, N. (2001) Superoxide anion generation via electron transfer oxidation of catechin dianion by molecular oxygen in an aprotic medium. *Chem. Lett.* 1152−1153.

(24) Fukuhara, K., Nakanishi, I., Kansui, H., Sugiyama, E., Kimura, M., Shimada, T., Urano, S., Yamaguchi, K., and Miyata, N. (2002) Enhanced radical scavenging activity of a planar catechin analogue. *J. Am. Chem. Soc.* **124**, 5952−5953.

(25) Guiso, M., Marra, C., and Cavarischia, C. (2001) Isochromans from 2 (3′,4′ dihydroxy)phenylethanol. *Tetrahedron Lett.* **42**, 6531−6534.

(26) Frisch, M. J., Trucks, G. W., Schlegel, H. B., Scuseria, G. E., Robb, M. A., Cheeseman, J. R., Zakrzewski, V. G., Montgomery, J. A., Jr., Stratmann, R. E., Burant, J. C., Dapprich, S., Millam, J. M., Daniels, A. D., Kudin, K. N., Strain, M. C., Farkas, O., Tomasi, J., Barone, V., Cossi, M., Cammi, R., Mennucci, B., Pomelli, C., Adamo, C., Clifford, S., Ochterski, J., Petersson, G. A., Ayala, P. Y., Cui, Q., Morokuma, K., Malick, D. K., Rabuck, A. D., Raghavachari, K., Foresman, J. B., Cioslowski, J., Ortiz, J. V., Baboul, A. G., Stefanov, B. B., Liu, G., Liashenko, A., Piskorz, P., Komaromi, I., Gomperts, R., Martin, R. L., Fox, D. J., Keith, T., Al Laham, M. A., Peng, C. Y., Nanayakkara, A., Gonzalez, C., Challacombe, M., Gill, P. M. W., Johnson, B., Chen, W., Wong, M. W., Andres, J. L., Gonzalez, C., Head Gordon, M., Replogle, E. S., and Pople, J. A. (1998) *Gaussian 98 (Revision A.7)* Gaussian, Inc., Pittsburgh, PA.

(27) Baerends, E. J., Ellis, D. E., and Ros, P. (1973) Self consistent Molecular Hartree−Fock−Slater Calculations I. The Computational Procedure. *Chem. Phys.* **2**, 41−51.

(28) te Velde, G., and Baerends, E. J. (1992) Numerical integration for polyatomic systems. *J. Comput. Phys.* **99**, 84−98.

(29) Vosko, S. H., Wilk, L., and Nusair, M. (1980) Accurate spin dependent electron liquid correlation energies for local spin density calculations: a critical analysis. *Can. J. Phys.* **58**, 1200−1205.

(30) Becke, A. D. (1988) Density functional exchange energy approximation with correct asymptotic behavior. *Phys. Rev. A* **38**, 3098−3100.

(31) Perdew, J. P. (1986) Density functional approximation for the correlation energy of the inhomogeneous electron gas. *Phys. Rev. B* **33**, 8822−8824.

(32) Perdew, J. P. (1986) Erratum: Density functional approximation for the correlation energy of the inhomogeneous electron gas. *Phys. Rev. B* **34**, 7406.

(33) Versluis, L., and Ziegler, T. (1988) The determination of molecular structures by density functional theory. The evaluation of analytical energy gradients by numerical integration. *J. Chem. Phys.* **88**, 322−328.

(34) Slabbert, N. P. (1977) Ionisation of some flavanols and dihydroflavonols. *Tetrahedron* **33**, 821−824.

(35) Stewart, J. J. P. (1989) Optimization of parameters for semiempirical methods. II. Applications. *J. Comput. Chem.* **10**, 221−264.

(36) Babcock, G. T., El Deeb, M. K., Sandusky, P. O., Whittaker, M. M., and Whittaker, J. W. (1992) Electron paramagnetic resonance and electron nuclear double resonance spectroscopies of the radical site in galactose oxidase and of thioether substituted phenol model compounds. *J. Am. Chem. Soc.* **114**, 3727−3734.

(37) Bagchi, R. N., Bond, A. M., Scholz, F., and Stösser, R. (1989) Characterization of the ESR spectrum of the superoxide anion in the liquid phase. *J. Am. Chem. Soc.* **111**, 8270−8271.

(38) Laughton, M. J., Halliwell, B., Evans, P. J., and Hoult, J. R. S. (1989) Antioxidant and prooxidant actions of the plant phenolics quercetin, gossypol and myricetin. Effects on lipid peroxidation, hydroxyl radical generation and bleomycin dependent damage to DNA. *Biochem. Pharmacol.* **38**, 2859−2865.

(39) Cao, G., Sofic, E., and Prior, R. (1997) Antioxidant and prooxidant behavior of flavonoids: structure activity relationships. *Free Radical Biol. Med.* **22**, 749−760.

(40) Metodiewa, D., Jaiswal, A. K., Cenas, N., Dickancaité, E., and Segura Aguilar, J. (1999) Quercetin may act as a cytotoxic prooxidant after its metabolic activation to semiquinone and quinoidal product. *Free Radical Biol. Med.* **26**, 107−116.

(41) Hodnick, W. F., Milosavljevic, E. B., Nelson, J. H., and Pardini, R. S. (1988) Electrochemistry of flabvonoids. Relationships between redox potentials, inhibition of mitochondrial respiration, and production of oxygen radicals by flavonoids. *Biochem. Pharmacol.* **37**, 2607−2611.

(42) Yamamoto, K., and Niki, E. (1988) Interaction of α tocopherol with iron: antioxidant and prooxidant effects of α tocopherol in the oxidation of lipids in aqueous dispersions in the presence of iron. *Biochim. Biophys. Acta* **958**, 19−23.

(43) Yamamoto, K., Takahashi, M., and Niki, E. (1987) Role of iron and ascorbic acid in the oxidation of methyl linoleate micelles. *Chem. Lett.* 1149−1152.

TX025581F

Available online at www.sciencedirect.com
SCIENCE DIRECT®
Chemico-Biological Interactions 146 (2003) 19–25
Chemico-Biological Interactions
www.elsevier.com/locate/chembioint

Structural activity relationship between *Salmonella*-mutagenicity and nitro-orientation of nitroazaphenanthrenes

Hiroshi Tokiwa [a,*], Nobuyuki Sera [b], Kiyoshi Fukuhara [c], Hideo Utsumi [d], Shigeki Sasaki [e], Naoki Miyata [e]

[a] *Department of Environmental Health Science, Kyushu Women's University, 1-1, Jiyugaoka, Yahatanishiku, Kitakyushu, Japan*
[b] *Department of Health Science, Fukuoka Institute of Health and Environmental Sciences, Fukuoka 818-01, Japan*
[c] *National Institute of Health Sciences, Setagaya-ku, Tokyo 158-8501, Japan*
[d] *Laboratory of Bio-function Analysis, Graduate School of Pharmaceutical Sciences, Kyushu University, 3-1-1 Maidashi, Higashi-ku, Fukuoka 812-8582, Japan*
[e] *Bioorganic and Synthetic Chemistry, Graduate School of Pharmaceutical Sciences, Kyushu University, 3-1-1 Maidashi, Higashi-ku, Fukuoka 812-8582, Japan*

Received 12 September 2002; accepted 27 March 2003

Abstract

Nitroazaphenanthrenes (NAphs) and their *N*-oxides (NAphOs) were synthesized as derivatives with nitrogen atoms in the 1, 4, and 9 positions of phenanthrene rings, and as nitrated derivatives substituted at the 1, 2, 3, 4, 5, 6, 7, and 8 positions of phenanthrene rings. To determine the structure activity relationship of these derivatives, all 19 isomers were bioassayed with *Salmonella* tester strains. NAphs substituted at the 4, 6, 7 and 8 positions were mutagenic for TA98, and 1-, 2-, and 3-N-9-AphOs, 6-N-1-AphO and 6-N-4-AphO were mutagenic for TA98 and TA100 without the S9 mix, while 5-N-1-AphO and 5-N-9-AphO were non- or weakly mutagenic. Nitrated derivatives, 6-N-4-Aph, 6-N-9-Aph, 6-N-1-AphO, and 6-N-4-AphO, were powerful mutagens for TA98 and TA100. Mutagenicity was enhanced by mutant strains producing nitroreductase, such as YG1021 and 1026, and by those producing *O*-acetyltransferase, such as YG1024 and 1029. Nitro derivatives substituted at positions 4 and 5 in the phenanthrene rings were perpendicular, while those at positions 2, 3, 6 and 7 were coplanar to the phenanthrene rings. NAphs substituted at the 1 and 8 positions were noncoplanar due to steric hindrance of the aromatic proton at the peri position. On the other hand, 1,5- and 1,8-dinitro-4-azaphenanthrenes showed high mutagenicity for strains TA98 and TA100 in the absence of the S9 mix, and were strongly enhanced by nitroreductase and *O*-acetyltransferase, over-producing mutants. Therefore, it was found that the mutagenic potency of NAphs and NAphOs was closely associated with the chemical properties and orientation of nitro substitution of aromatic rings.

Keywords: Nitroazaphenanthrenes; *Salmonella* mutagenicity; Nitro-orientation

* Corresponding author. Tel.: +81-693-3088; fax: +81-692-3245.
E-mail address: tokiwa@kwuc.ac.jp (H. Tokiwa).

0009-2797/03/$ - see front matter
doi:10.1016/S0009-2797(03)00070-X